

©Copyright 2014

Kelsey Vitense

Theoretical Impacts of Habitat Loss and Generalist Predation on Predator-Prey Cycles

Kelsey Vitense

A thesis submitted in partial fulfillment of the
requirements for the degree of

Master of Science

University of Washington

2014

Reading Committee:

James J. Anderson, Chair

Aaron J. Wirsing, Chair

Trevor Branch

Rebecca Tyson

Program Authorized to Offer Degree:
Quantitative Ecology and Resource Management

University of Washington

Abstract

Theoretical Impacts of Habitat Loss and Generalist Predation on Predator-Prey Cycles

Kelsey Vitense

Co-Chairs of the Supervisory Committee:
Research Professor James J. Anderson
Columbia Basin Research

Assistant Professor Aaron J. Wirsing
School of Environmental and Forest Sciences

Certain herbivores and their predators undergo high amplitude periodic fluctuations in abundance in northern latitudes but exhibit damped cyclic dynamics in their respective southern ranges. Generalist predation and habitat loss have been identified as two features of southern habitats that may contribute to the attenuation of cycles in southern latitudes. I used a reaction-diffusion-advection framework to investigate the relative and combined damping impacts of generalist predation and habitat loss with reaction terms taken from the May and Rosenzweig-MacArthur models. The models were parameterized using data from snowshoe hare and Canada lynx field studies to generate similar cyclic dynamics in the center of a single patch in the absence of generalist predation. I found that generalist predation has strong stabilizing effects for both models and may represent a threat to the persistence of specialized predators. The magnitude of cycle damping due to habitat loss depends on movement rates and model choice, but ultimately results in the loss of cycles. Differences in model carrying capacity may explain differences in model sensitivity to habitat loss, and cycle amplitude may or may not decrease monotonically with habitat loss, depending on model choice. Elevated generalist predation rates at patch edges and in matrix habitat hasten cycle attenuation in situations that lead to increased prey exposure to generalists, including small patch size, higher movement rates into the matrix, and increased prey density at patch edges. Habitat disturbances may therefore have myriad consequences

for cyclic systems depending in part on the nature of specialist predator-prey interactions and the extent to which the disturbances increase generalist access to prey. Field data that clarifies the relationships between habitat loss and fragmentation, generalist density and behavior, and cyclic activity would be invaluable in informing future modeling efforts.

TABLE OF CONTENTS

	Page
List of Figures	ii
List of Tables	v
Chapter 1: Theoretical Impacts of Habitat Loss and Generalist Predation on Predator-Prey Cycles	1
1.1 Introduction	1
1.2 Methods	4
1.3 Results	14
1.4 Discussion	24
Bibliography	33
Appendix A: Supplementary material	40
A.1 Spatial functions	40
A.2 Northern baseline dynamics	42
A.3 Type III functional response	45
A.4 Habitat loss and predator velocity	46
A.5 Habitat loss and diffusion ratio	48
A.6 Limit cycles at low diffusivity	50
Appendix B: Repository	52
B.1 Northern baseline dynamics and diffusion	52
B.2 Generalist predation and diffusion	53
B.3 Habitat loss and matrix velocity	54

LIST OF FIGURES

Figure Number	Page	
1.1	Prey logistic growth and specialist functional response for the May and R-M models. (a) Prey growth rate increases with prey density until the inflection point is reached at half the carrying capacity ($k/2$), then growth rate decreases as prey density rises and approaches k . (b) The specialist predator exhibits a Holling Type II functional response for both models. At low prey densities, the predation rate rises sharply with prey density. The specialist predator is eventually limited by its ability to process additional food at high prey densities, and the predation rate approaches its maximum, α . See Table 1.2 for parameter values.	10
1.2	Spatial reproduction, velocity, and generalist predation functions. Representative spatial functions are shown for a center patch of length 20 (2 km). Dotted lines indicate patch boundaries. (a) Prey reproduction function. (b) Specialist predator and prey velocity function. (c) Matrix-based generalist predation function at matrix predation rate, $\gamma_{mat} = 1.0$ prey/ha/yr. See Appendix A.1 for function details.	13
1.3	May and R-M time series at high diffusivity. The last 30 years of the 500 year simulated time series as measured in the center of a single patch at high diffusivity ($D_L = 20$ ha/yr) with no generalist predation. Parameter values are as shown in Table 1.2.	15
1.4	Bifurcation plots for generalist predation and habitat loss. (a) May and (c) R-M prey cycle maximum and minimum plotted as a function of γ at high diffusivity. Low diffusivity plots look almost identical. (b) May and (d) R-M prey cycle maximum and minimum plotted as a function of habitat loss percentage at low and high diffusivity. Oscillations cease where the maximum and minimum lines coalesce. The star denotes a max/min amplitude ≤ 1.5 , which is the threshold used in Tyson et al. (2010) for cyclicity. Cycles are effectively lost at $\gamma = 0.25$ for May and $\gamma = 1.0$ for R-M at both low and high diffusivity. May cycles stop at 95% habitat loss at low diffusivity and 75% loss at high diffusivity. R-M cycles stop at 80% habitat loss at low diffusivity and 35% loss at high diffusivity.	17

1.5	Limit cycles at varying maximum generalist predation rate and percent habitat loss at high diffusivity. Panels (a) and (c) show the effect of increasing γ on the predator-prey limit cycles for the May and R-M models, respectively, while panels (b) and (d) show the impact of habitat loss. Prey density is plotted on the x -axis, and predator density is located on the y -axis. Stable equilibrium points are represented by single points. See Appendix A.6 for low diffusivity cycles.	18
1.6	May model prey amplitude contour plots for spatially uniform and matrix-based generalists. Contour lines represent prey amplitude at the center of prey habitat computed as the ratio of cycle maximum over minimum. Panels (a) and (b) show the effect of simultaneously increasing habitat loss and spatially uniform generalist density at low and high diffusivity, respectively. Panels (c) and (d) show the effects of increasing habitat loss and matrix-based generalist densities. Percent habitat loss is shown on the x -axis, while the y -axis is the value of γ at the center of the patch, whether predation is uniform or matrix-based.	20
1.7	R-M model prey amplitude contour plots for spatially uniform and matrix-based generalists. Panels (a)-(d) are the same as in Fig.1.6, with the exception that the range of γ is twice as large.	21
1.8	Spatial profiles of peak densities for May and R-M prey. Thick solid lines indicate the boundaries of the spatial domain. Dotted lines indicate the patch boundaries, where the center patch is 3.2 km in length. Colored solid lines show peak prey densities in space for the two models.	23
A.1	May and R-M time series at low diffusivity. The last 30 years of the 500 year simulated time series as measured in the center of a single patch at low diffusivity ($D_L = 2$ ha/yr) with no generalist predation. Parameter values are as shown in Table 1.2.	42
A.2	Generalist Type III functional response. The effect of increasing the maximum generalist predation rate, γ , on the Type III response while holding the half-saturation constant, η , fixed at 1.25 prey/ha.	45
A.3	Bifurcation plots with and without predator velocity at low diffusivity. (a) May and (b) R-M prey cycle maximum and minimum plotted as a function of habitat loss percentage, where $V_L = 0$ is without a predator velocity function, and $V_L \neq 0$ is with a predator velocity function. Oscillations cease where the maximum and minimum lines coalesce. The star denotes a max/min amplitude ≤ 1.5 . Demographic parameter values are in Table 1.2.	47
A.4	Bifurcation plots with and without predator velocity at high diffusivity. Same as Fig. A.3 but at high diffusivity.	47

A.5	Bifurcation plots at varying diffusion ratios at low diffusivity. (a) May and (b) R-M prey cycle maximum and minimum plotted as a function of habitat loss percentage, where $D = \frac{D_H}{D_L}$ and $D_L = 2$ ha/yr. Oscillations cease where the maximum and minimum lines coalesce. The star denotes a max/min amplitude ≤ 1.5 . Demographic parameter values are in Table 1.2.	49
A.6	Bifurcation plots at varying diffusion ratios at high diffusivity. Same as Fig. A.5 but at high diffusivity ($D_L = 20$ ha/yr). The maximum for $D = .25$ is slightly cut off in panel (a) for the prey density limits used in all other figures.	49
A.7	Limit cycles at varying maximum generalist predation rate and percent habitat loss at low diffusivity. Panels (a) and (c) show the effect of increasing γ on the predator-prey limit cycles for the May and R-M models, respectively, while panels (b) and (d) show the impact of habitat loss. Prey density is plotted on the x -axis, and predator density is located on the y -axis. Stable equilibrium points are represented by single points.	51
B.1	Bifurcation plots for two velocity functions at low diffusivity. (a) May and (b) R-M prey cycle maximum and minimum plotted as a function of habitat loss percentage, where ‘Whole patch’ refers to the non-zero velocity function over the whole matrix, and ‘Half patch’ refers to the function used in this thesis with zero velocity on the outer halves of the matrix. Oscillations cease where the maximum and minimum lines coalesce. The star denotes a max/min amplitude ≤ 1.5 . Demographic parameter values are in Table 1.2.	55
B.2	Bifurcation plots for two velocity functions at high diffusivity. Same as Fig. B.1 but at high diffusivity.	55

LIST OF TABLES

Table Number	Page
1.1 Scenario table. Parameters listed are modifications to the full model equations (1.2-1.5).	8
1.2 Fixed demographic parameter values for the May and R-M models, along with units and biological interpretations. Parameter ranges and specific values were taken from field studies in Alberta and the Southern Yukon and mathematical modeling studies (O’Donoghue et al. 1998, Ruggiero et al. 2000, Hodges et al. 2001, King and Schaffer 2001, Krebs et al. 2001 <i>b</i> , Strohm and Tyson 2009, Tyson et al. 2010).	9
A.1 Prey and predator cycle attributes for the May and R-M models on a single patch at high diffusivity. Attributes are measured in the center of the single patch without generalist predators over the last 30 years of a 500 year simulated time series. Prey maximums and minimums have units prey/ha and predator maximums and minimums have units predators/10 km ² . Amplitudes computed as the difference between maximums and minimums inherit the corresponding units. Amplitudes computed as the quotient between maximums and minimums are dimensionless. Period is measured in years. Cycle attributes are shown for prey/predator diffusion ratio $D = \frac{D_H}{D_L} = .50$ and a “high” predator diffusivity of $D_L = 20$ ha/yr.	43
A.2 Prey and predator cycle attributes for the May and R-M models on a single patch at low diffusivity. Attributes are measured in the center of the single patch without generalist predators over the last 30 years of a 500 year simulated time series. Units are as described in Table A.1 above. Cycle attributes are shown for prey/predator diffusion ratio $D = \frac{D_H}{D_L} = .50$ and a “low” predator diffusivity of $D_L = 2$ ha/yr.	44
B.1 Impacts of increasing predator diffusivity on May prey and predator cycle attributes in the center of a single patch without generalist predation at $D = \frac{D_H}{D_L} = .75$ and $D = .5$. Parameter values can be found in Table 1.2. (diff) denotes amplitude computed as the difference between maximum and minimum, and (ratio) denotes amplitude computed as the ratio of maximum over minimum.	52

B.2 Impacts of increasing predator diffusivity on R-M prey and predator cycle attributes in the center of a single patch without generalist predation at $D = \frac{D_H}{D_L} = .75$ and $D = .5$. Parameter values can be found in Table 1.2. (diff) denotes amplitude computed as the difference between maximum and minimum, and (ratio) denotes amplitude computed as the ratio of maximum over minimum. 53

B.3 Critical maximum generalist predation rates for cyclicity for the May and R-M models as diffusivity increases at prey/predator diffusion ratios $D = \frac{D_H}{D_L} = .75$ and $D = .5$. (diff) denotes amplitude computed as the difference between maximum and minimum, where γ_s is the maximum generalist predation rate at which the difference is ≤ 0.1 . (ratio) denotes amplitude computed as the ratio of maximum over minimum, where γ_s is the maximum generalist predation rate at which the ratio is ≤ 1.5 54

ACKNOWLEDGMENTS

I would like to thank the members of my committee for their guidance and support at every stage of my thesis. I am greatly indebted to my two advisors, Jim Anderson and Aaron Wirsing, for helping me grow as a scientist, modeler, and writer. Jim's humor throughout the writing process and Aaron's constant positivity and enthusiasm were saving graces. Trevor Branch never failed to ask challenging and thought-provoking questions, and his R graphics course proved to be very useful for this project. Rebecca Tyson spent many hours in discussions with me about this work, and her generous and communal approach to science is truly commendable.

The Anderson, Gallucci, and Wirsing labs provided outstanding feedback on half-baked ideas, figures, and presentations. My work improved leaps and bounds at every meeting with these students, and I feel privileged to have had them as peers. I am also incredibly grateful to Shaun Strohm for getting me started with code and a modeling framework for this study. This project was greatly expedited because of his willingness to share his work.

Thanks to the Bonneville Power Administration and Aaron Wirsing for helping to fund this project. Additionally, this work would not have been possible without TA support from the Center for Quantitative Science. My experiences as a TA were invaluable in building my communication skills during my degree, and I am very thankful for the opportunity.

I cannot overstate how essential the love and support I receive from my family has been and continues to be in my life. It is inconceivable that I could have made it this far without them. I am also so thankful for my wonderful friends who kept me sane the last three years. They know who they are.

Finally, I would like to thank KEXP for providing much of the soundtrack to my thesis, as well as the excellent musicians in this world who brighten every day of my life.

DEDICATION

I dedicate this thesis to Elaine Moes and David Romano. The encouragement and affirmation I received from these two teachers set me on the path to mathematics and graduate school. I hope I might impact the lives of others as positively as they did mine.

Chapter 1

THEORETICAL IMPACTS OF HABITAT LOSS AND GENERALIST PREDATION ON PREDATOR-PREY CYCLES**1.1 Introduction**

The multiannual population cycles of certain mammals and their predators in northern latitudes have been studied extensively over the last century (Elton and Nicholson 1942, Keith 1990, Akçakaya 1992, King and Schaffer 2001, Korpimäki et al. 2004, Tyson et al. 2010, Krebs 2011). The importance of cyclic herbivores, such as snowshoe hares (*Lepus americanus*) and brown lemmings (*Lemmus trimucronatus*), to tundra and boreal ecosystems lies at the heart of this interest in oscillatory population dynamics (Krebs 2011). These species are major food resources for many predators in addition to being consumers of large amounts of plant material. Hypotheses for the causes of population cycles have invoked sunspots, weather, forest fires, stress, food shortage, plant defenses, and parasites (Akçakaya 1992). While some of these features likely affect population densities, predation is now widely accepted as a key driver of cyclic fluctuations (Akçakaya 1992, Turchin 2003, Korpimäki et al. 2004, Krebs 2011). However, less attention has been given to the cause of the observed reductions in amplitude and densities of cyclic species in their respective southern ranges (Akçakaya 1992), and it is this phenomenon to which this study is devoted.

The snowshoe hare and its specialist predator, the Canada lynx (*Lynx canadensis*), will serve as a case study due to their use as a classic example of oscillatory predator-prey dynamics and for the abundance of available time series data. Additionally, the Canada lynx is listed as a threatened species in the lower 48 states and is therefore notable as a conservation concern.

Hare populations in northern boreal forests are famous for their dramatic cyclic fluctuations in abundance, characterized by a period of eight to 11 years and amplitudes that

are often 10- to 25-fold (Hodges 2000*a*). In contrast to populations in the north, the oscillatory dynamics of hare and lynx populations at southern latitudes are much attenuated (Keith 1990), with hare cycle amplitudes usually on the lower end of the two- to 25-fold observed range (Hodges 2000*b*). Two factors that may contribute to the damped dynamics of snowshoe hares and other species in their respective southern latitudes are landscape fragmentation and generalist predation. Suitable prey habitat in southern latitudes is naturally patchier or more fragmented due to human influences (Howell 1923, Wolff 1980, Keith et al. 1993, Agee 2000), and this reduction in reproductive habitat may not allow for the rates of population increase necessary to produce high amplitude cycles. The density and diversity of numerically stable generalist predators is also higher in the south, and prey are therefore consistently removed by predators that do not cycle along with them (Hanski et al. 1991, Erlinge et al. 1992, Klemola et al. 2002).

Moreover, with increased landscape disturbance, generalist predators are able to use areas occupied by specialists that were previously inaccessible, so fragmentation and increased abundance of generalists are expected to occur simultaneously (Buskirk 2000). Generalist predators are thought to benefit from fragmented landscapes through increased visibility and mobility in disturbed areas, access to a broad range of food sources, and exploitation of edge habitats (Andrews 1990, Harrison and Bruna 1999, Buskirk 2000, Gehring and Swihart 2003). Indeed, Andrén et al. (1985) observed that the density of generalist corvid birds was higher south of the boreal zone in Sweden where cycles of tetraonid birds disappear, and was positively correlated with dummy nest predation rate, fragmentation degree of forests, and proportion of agricultural lands. Further, Andrén and Angelstam (1988) found that dummy nest predation rates in Sweden were highest in farmland habitat, with an increase in predation extending into neighboring forest habitat leveling off 200-500m from the edge. Other studies have found edge-related increases in predation ranging from 50m to 4km (Patton 1994, Batáry and Báldi 2004, Storch et al. 2005) from the edge. Additionally, Wilcove (1985) observed elevated nest predation rates on very small forest fragments and on patches closer to suburban areas. Accordingly, some snowshoe hare studies have found increased predation in open areas with reduced cover (Dolbeer 1975, Sievert and Keith 1985, Griffin and Mills 2009), while others have found predation to be very high on small patches of

habitat in highly fragmented landscapes (Keith et al. 1993, Wirsing et al. 2002).

These observations of spatial heterogeneity in predation rates suggests that there is strong potential for generalist predators to interact with forest fragmentation to influence cycles, but these effects and the impacts on threatened species like the lynx are currently unknown (McKelvey et al. 2000). Authors have made use of the wealth of data provided by the Hudson's Bay Company's well-known records of hare and lynx fur returns (Elton and Nicholson 1942, MacLulich 1957) and intensive field studies in Rochester, Alberta (Keith 1990) and Kluane Lake, Yukon (Krebs et al. 2001*a*) to propose and parameterize mechanistic models for northern hare-lynx cycles (Akçakaya 1992, Ives and Murray 1997, King and Schaffer 2001, Tyson et al. 2010). In contrast, no southern field studies have exceeded four years in duration, and studies have occurred over such a wide variety of habitats and climates that generalizations are difficult to make (Murray 2000).

Though data are lacking in the south, theorists have taken models similar to those fit to northern data and perturbed the cycles according to environmental parameters and forms of predation that are suspected to be different in the south to explore conditions that disrupt cycles. For instance, Hanski et al. (1991) used differential equations to show that generalist predation has a strong damping impact on predator-prey cycles characteristic of small rodents and mustelids in Fennoscandia. Taylor et al. (2013) used the same model to show that a shortened breeding season in southern latitudes results in shorter cycle period. In an individual-based simulation study, Szwabiński and Pękalski (2006) found that habitat loss weakened stochastically generated fluctuations in predator and prey abundance. Strohm and Tyson (2009) further demonstrated that habitat loss decreases the amplitude of hare-lynx cycles for four different mechanistic models. While some theoretical work has been done to investigate how habitat fragmentation and generalist predation work in concert to affect predator-prey dynamics (Schneider 2001, Swihart et al. 2001), such studies have not addressed population cycles.

In this chapter, I investigate the effects of generalist predation and habitat loss on predator-prey cycles using two models with different functional forms. I first explore the relative effects of generalist predation and habitat loss to establish how each works to damp cycles and to compare model responses. I then examine the combined effects by considering

both spatially uniform and matrix-based generalist predation. This comparison in spatial patterns will provide insight into whether and when spatial differences in predation are important to consider for both future field work and modeling efforts.

1.2 Methods

Models

Following Strohm and Tyson (2009), I used reaction-diffusion-advection models of the following form to describe population dynamics:

$$\frac{\partial n}{\partial t} = D \frac{\partial^2 n}{\partial x^2} + \frac{\partial[V(x)n]}{\partial x} + f(n, x), \quad (1.1)$$

where $n = n(x, t)$ is the population density at location x at time t ; D is a spatially uniform diffusion coefficient; $V(x)$ is spatially varying velocity; and $f(n, x)$ is the reaction term describing changes in population density that are not due to movement of individuals (e.g. reproduction, natural mortality, predation). For simplicity, movement occurs in one spatial dimension, and similarly, population density varies in just one dimension. A system of partial differential equations (PDEs) was used to model the dynamics of a specialist predator and its prey, and reaction terms were taken from two different models, the May (2001) and Rosenzweig-MacArthur models (Rosenzweig and MacArthur 1963).

The full equations for the May model are as follows:

$$\frac{\partial H}{\partial t} = D_H \frac{\partial^2 H}{\partial x^2} + \frac{\partial[V(x)H]}{\partial x} + r(x)H \left(1 - \frac{H}{k}\right) - \frac{\alpha HL}{\beta + H} - \frac{\gamma(x)H^2}{H^2 + \eta^2}, \quad (1.2)$$

$$\frac{\partial L}{\partial t} = D_L \frac{\partial^2 L}{\partial x^2} + \frac{\partial[V(x)L]}{\partial x} + sL \left(1 - \frac{qL}{H}\right), \quad (1.3)$$

where H is prey density and L is predator density. This model includes logistic growth for both prey and predator, where the predator's carrying capacity is proportional to prey density (H/q in Eq. (1.3)). As prey density decreases, predator territory size must therefore increase, consistent with observations of lynx (Ward and Krebs 1985). This form of the

carrying capacity also implies that predators may persist at very low prey densities, which is a common criticism of the May model (Turchin 2003), but the model was investigated due to its prevalence in the literature on cycles (Turchin and Hanski 1997, Strohm and Tyson 2012, Taylor et al. 2013) and because it has been fit to field data from the Yukon (Tyson et al. 2010). The final piece of the May model is Holling's Type II hyperbolic functional response for the predator in Eq. (1.3), which is the form firmly established for specialist predators (Holling 1959, Turchin 2003).

Following Turchin and Hanski (1997), a Holling Type III functional response was used to incorporate generalist predation in the prey equation (Holling 1959). The density of generalist predators was assumed to be independent of prey density, with ample alternative prey available when the focal prey density is low. The Type III functional response is sigmoidal in shape and describes the prey switching behavior of generalist predators. As prey density initially rises from very low densities, the predation rate of generalists increases at an exponential rate as the predators switch from other prey items and become more efficient at finding and killing the increasingly abundant prey species. The generalists are eventually limited by their capacity to process additional prey items at high prey density, and the predation rate approaches its maximum, γ .

The full equations for the Rosenzweig-MacArthur (R-M) model are

$$\frac{\partial H}{\partial t} = D_H \frac{\partial^2 H}{\partial x^2} + \frac{\partial[V(x)H]}{\partial x} + r(x)H \left(1 - \frac{H}{k}\right) - \frac{\alpha HL}{\beta + H} - \frac{\gamma(x)H^2}{H^2 + \eta^2}, \quad (1.4)$$

$$\frac{\partial L}{\partial t} = D_L \frac{\partial^2 L}{\partial x^2} + \frac{\partial[V(x)L]}{\partial x} + \frac{\chi\alpha HL}{\beta + H} - \delta L. \quad (1.5)$$

The prey equation for the R-M model (1.4) is the same as the prey equation for the May model (1.2). The predator equation (1.5), however, is different. Namely, the parameter χ is the prey-to-predator conversion ratio, and predator growth is therefore proportional to the loss of prey in Eq. (1.4). Additionally, the predators die at an exponential rate in the absence of prey.

Scenarios

To investigate the relative and combined effects of generalist predation and habitat loss, I explored four different “scenarios” by manipulating certain parameters in the full models (See Table 1.1). For each scenario, solutions were obtained numerically using the Matlab PDE solver for one spatial dimension, *pdepe*. The solver discretizes the system of PDEs over the user-defined spatial grid, and the resulting ODEs are solved with *ode15s*, a variable-order solver for stiff problems based on numerical differentiation formulas (Shampine and Reichelt 1997). Both models have 4 km spatial domains, where $-20 \leq x \leq 20$. Zero-flux boundary conditions and the same uniform initial conditions were used for both models in all scenarios:

$$\frac{\partial H(-20, t)}{\partial t} = 0, \quad \frac{\partial H(20, t)}{\partial t} = 0, \quad \frac{\partial L(-20, t)}{\partial t} = 0, \quad \frac{\partial L(20, t)}{\partial t} = 0. \quad (1.6)$$

$$H(x, 0) = 5, \quad L(x, 0) = 0.01. \quad (1.7)$$

For each scenario, solutions were simulated for 500 years to allow for complete decay of transients, and the last 30 years of the simulation were recorded.

1.2.1 Scenario 1: Northern baseline

First, I established specialist predator-prey cycles characteristic of hare-lynx cycles across the boreal forests of Canada and Alaska by considering a single patch without generalist predators (Scenario 1 in Table 1.1).

The equations for the May model are reduced to

$$\frac{\partial H}{\partial t} = D_H \frac{\partial^2 H}{\partial x^2} + r(x)H \left(1 - \frac{H}{k}\right) - \frac{\alpha HL}{\beta + H}, \quad (1.8)$$

$$\frac{\partial L}{\partial t} = D_L \frac{\partial^2 L}{\partial x^2} + sL \left(1 - \frac{qL}{H}\right), \quad (1.9)$$

and the R-M equations are reduced to

$$\frac{\partial H}{\partial t} = D_H \frac{\partial^2 H}{\partial x^2} + r(x)H \left(1 - \frac{H}{k}\right) - \frac{\alpha HL}{\beta + H}, \quad (1.10)$$

$$\frac{\partial L}{\partial t} = D_L \frac{\partial^2 L}{\partial x^2} + \frac{\chi \alpha HL}{\beta + H} - \delta L. \quad (1.11)$$

Table 1.2 lists parameter values, units, and biological meanings. The parameters for the May model are the same as the default values used in Tyson et al. (2010) and Strohm and Tyson (2009). These values are based on observed ranges from field studies in Alberta and the southern Yukon (O’Donoghue et al. 1998, Ruggiero et al. 2000, Hodges et al. 2001, King and Schaffer 2001, Krebs et al. 2001*b*) and were chosen to generate hare-lynx cycles with maximums, minimums, and period as close as possible to those observed at Kluane Lake in the Yukon (Tyson et al. 2010). The parameters for the Rosenzweig-MacArthur model were selected to achieve similar prey and predator densities as the parameterized May model, again within ranges taken from the literature for ecological fidelity. I used an alternate parameterization of the R-M model compared to that of Strohm and Tyson (2009), where the prey intrinsic growth rate, r , is the same for both models because this parameter is manipulated in the habitat loss analysis below. Additionally, forcing the same r means prey growth rates are indistinguishable at low prey densities (Fig. 1.1a). The prey intrinsic growth rate for both models varies spatially over the single patch, consistent with the methods of Strohm and Tyson (2009) and the multiple patch analyses of Scenarios 3-5 (Fig. 1.2a). I also adjusted the parameters for the predator functional response to be as similar as possible (Fig. 1.1b). Two sets of diffusion coefficients were used for both models, deemed “low” and “high” diffusivity, where the predator diffuses at $D_L = 2$ and 20 ha/yr, respectively, with prey diffusivity at half the predator’s rate.

Aside from the form of the predator equations, the biggest difference between the two models lies in the prey carrying capacity. The carrying capacity for the R-M model was lowered from 8 prey/ha to 4 prey/ha to bring the prey cycle maximum close to the May cycle maximum. The R-M prey growth rate above its inflection point of 2 prey/ha is therefore much lower than the May prey growth rate (Fig. 1.1a).

Table 1.1: Scenario table. Parameters listed are modifications to the full model equations (1.2-1.5).

Habitat loss	Generalist predation	
	Absent	Present
Absent	1. Northern baseline $V(x) = 0$ $r(x) = \text{Fig. 1.2a (no matrix)}$ $\gamma(x) = 0$	2. Generalist Predation $V(x) = 0$ $r(x) = \text{Fig. 1.2a (no matrix)}$ $\gamma(x) = \gamma$
Present	3. Habitat loss $V(x) = \text{Fig. 1.2b}$ $r(x) = \text{Fig. 1.2a}$ $\gamma(x) = 0$	4. Generalist predation + habitat loss $V(x) = \text{Fig. 1.2b}$ $r(x) = \text{Fig. 1.2a}$ a. Spatially uniform generalists $\gamma(x) = \gamma$ b. Matrix-based generalists $\gamma(x) = \text{Fig. 1.2b}$

Table 1.2: Fixed demographic parameter values for the May and R-M models, along with units and biological interpretations. Parameter ranges and specific values were taken from field studies in Alberta and the Southern Yukon and mathematical modeling studies (O'Donoghue et al. 1998, Ruggiero et al. 2000, Hodges et al. 2001, King and Schaffer 2001, Krebs et al. 2001*b*, Strohm and Tyson 2009, Tyson et al. 2010).

Parameter	Biological Meaning	Units	May	R-M
r	Prey intrinsic growth rate	$\frac{1}{\text{year}}$	1.75	1.75
k	Prey carrying capacity	$\frac{\text{prey}}{\text{ha}}$	8	4
α	Specialist saturation kill rate	$\frac{\text{prey}}{\text{predator} \times \text{yr}}$	505	550
β	Specialist half-saturation constant	$\frac{\text{prey}}{\text{ha}}$	0.3	0.5
s	Specialist intrinsic growth rate	$\frac{1}{\text{year}}$	0.85	–
q	Prey biomass required per specialist	$\frac{\text{prey}}{\text{predator}}$	212	–
χ	Prey-specialist conversion rate	$\frac{\text{predators}}{\text{prey}}$	–	0.005
δ	Specialist death rate in absence of prey	$\frac{1}{\text{year}}$	–	2.0
γ	Generalist saturation kill rate	$\frac{\text{prey}}{\text{ha} \times \text{yr}}$	0-25	0-25
η	Generalist half-saturation constant	$\frac{\text{prey}}{\text{ha}}$	1.25	1.25

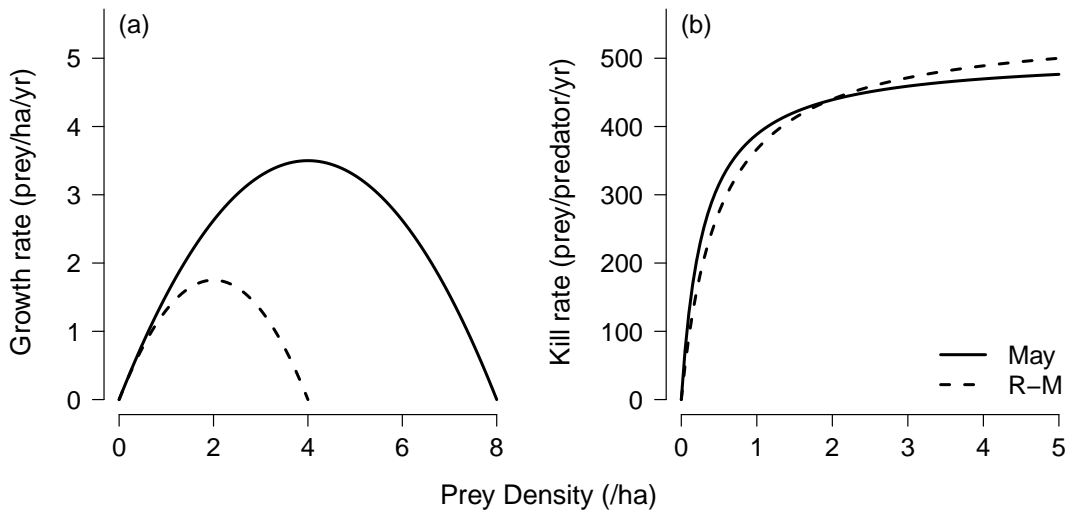


Figure 1.1: Prey logistic growth and specialist functional response for the May and R-M models. (a) Prey growth rate increases with prey density until the inflection point is reached at half the carrying capacity ($k/2$), then growth rate decreases as prey density rises and approaches k . (b) The specialist predator exhibits a Holling Type II functional response for both models. At low prey densities, the predation rate rises sharply with prey density. The specialist predator is eventually limited by its ability to process additional food at high prey densities, and the predation rate approaches its maximum, α . See Table 1.2 for parameter values.

1.2.2 Scenario 2: Generalist predation

The aim of this scenario is to explore the damping impact of generalist predation for the two models. To simulate a geographical gradient in generalist predation, the Type III generalist response was returned to the prey equations (Scenario 2 in Table 1.1). For the May model, the equations become

$$\frac{\partial H}{\partial t} = D_H \frac{\partial^2 H}{\partial x^2} + r(x)H \left(1 - \frac{H}{k}\right) - \frac{\alpha HL}{\beta + H} - \frac{\gamma H^2}{H^2 + \eta^2}, \quad (1.12)$$

$$\frac{\partial L}{\partial t} = D_L \frac{\partial^2 L}{\partial x^2} + sL \left(1 - \frac{qL}{H}\right), \quad (1.13)$$

and the RDEs for the R-M model become

$$\frac{\partial H}{\partial t} = D_H \frac{\partial^2 H}{\partial x^2} + r(x)H \left(1 - \frac{H}{k}\right) - \frac{\alpha HL}{\beta + H} - \frac{\gamma H^2}{H^2 + \eta^2}, \quad (1.14)$$

$$\frac{\partial L}{\partial t} = D_L \frac{\partial^2 L}{\partial x^2} + \frac{\chi \alpha HL}{\beta + H} - \delta L. \quad (1.15)$$

The half-saturation constant was fixed at $\eta = 1.25$ prey/ha for both models, which is the value used in Tyson et al. (2010). The generalist saturation kill rate, γ , was increased uniformly over the single patch while holding the other parameters at their northern baseline values. Estimates from the Klwane Project (Hodges et al. 2001) put γ between .1-2 prey/ha/year, but values up to 25 prey/ha/year were investigated to determine not only levels of predation that stabilize dynamics, but also predation rates that cause extirpation. For the purpose of this analysis, an increase in γ was viewed as an increase in generalist density.

1.2.3 Scenario 3: Habitat loss

The intent of this scenario is to explore the effect of the north-south habitat loss gradient on cyclic activity. I used a three patch domain consisting of a single patch of suitable prey

habitat surrounded by two patches of inhospitable habitat (i.e. matrix habitat). Adding in the velocity term and removing the generalist term (Scenario 3 in Table 1.1), the May equations become

$$\frac{\partial H}{\partial t} = D_H \frac{\partial^2 H}{\partial x^2} + \frac{\partial[V(x)H]}{\partial x} + r(x)H \left(1 - \frac{H}{k}\right) - \frac{\alpha HL}{\beta + H}, \quad (1.16)$$

$$\frac{\partial L}{\partial t} = D_L \frac{\partial^2 L}{\partial x^2} + \frac{\partial[V(x)L]}{\partial x} + sL \left(1 - \frac{qL}{H}\right), \quad (1.17)$$

while the R-M equations become

$$\frac{\partial H}{\partial t} = D_H \frac{\partial^2 H}{\partial x^2} + \frac{\partial[V(x)H]}{\partial x} + r(x)H \left(1 - \frac{H}{k}\right) - \frac{\alpha HL}{\beta + H}, \quad (1.18)$$

$$\frac{\partial L}{\partial t} = D_L \frac{\partial^2 L}{\partial x^2} + \frac{\partial[V(x)L]}{\partial x} + \frac{\chi \alpha HL}{\beta + H} - \delta L. \quad (1.19)$$

Consistent with the methods of Strohm and Tyson (2009), the prey reproduction function, $r(x)$, is now positive only in the prey habitat patch (Fig. 1.2a), and the velocity function, $V(x)$, is zero inside of the prey habitat patch but pulls animals towards the patch if they are in the matrix but still near the patch (Fig. 1.2b). The size of the habitat patch was reduced in 200 m increments while increasing the size of the matrix to maintain constant domain length. The reproduction and velocity functions were scaled so that the growth rate attains its maximum, $r = 1.75$, precisely in the center of the patch, and the maximum velocity of ± 100 m/yr is always attained, regardless of patch size.

1.2.4 Scenario 4: Generalist predation and habitat loss combined

In Scenario 4, the combined effects of generalist predation and habitat loss on cycles were investigated in two different fashions. First, the last two analyses were done simultaneously, where the length of the habitat patch was steadily decreased at varying levels of γ , with γ being uniform in space (Scenario 4a). The prey equations for both models now contain both advection and generalist terms, where $\gamma(x) = \gamma$:

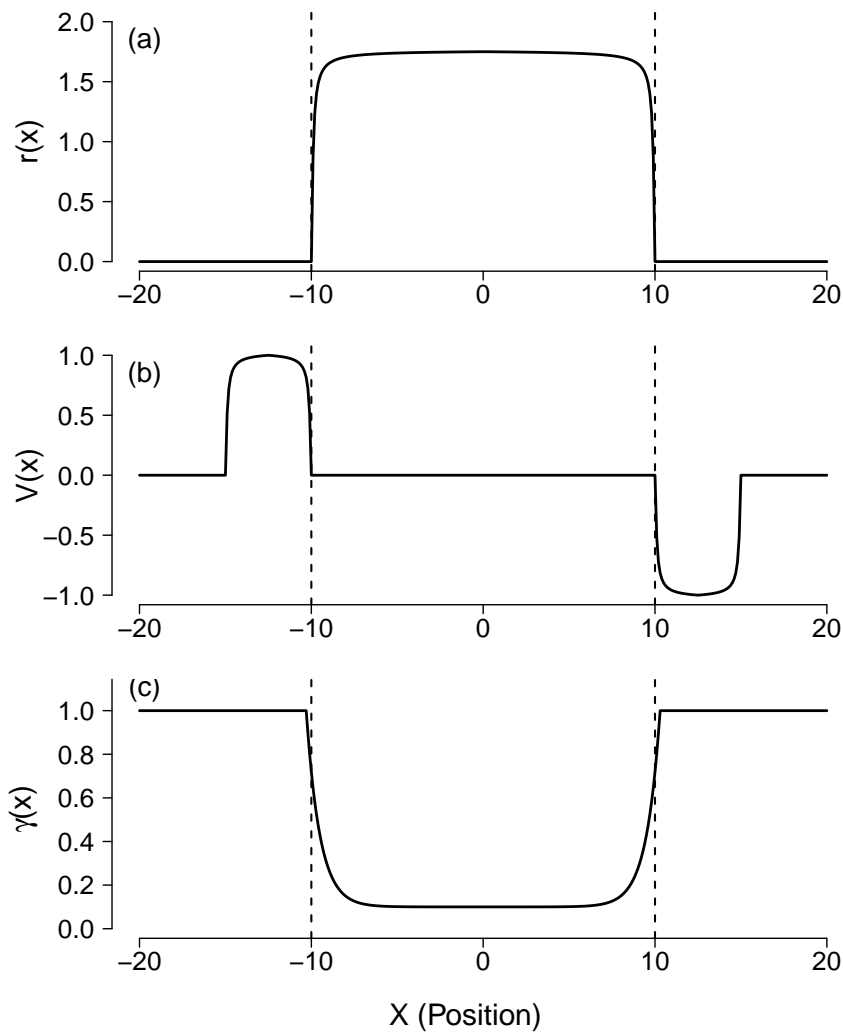


Figure 1.2: Spatial reproduction, velocity, and generalist predation functions. Representative spatial functions are shown for a center patch of length 20 (2 km). Dotted lines indicate patch boundaries. (a) Prey reproduction function. (b) Specialist predator and prey velocity function. (c) Matrix-based generalist predation function at matrix predation rate, $\gamma_{mat} = 1.0$ prey/ha/yr. See Appendix A.1 for function details.

$$\frac{\partial H}{\partial t} = D_H \frac{\partial^2 H}{\partial x^2} + \frac{\partial[V(x)H]}{\partial x} + r(x)H \left(1 - \frac{H}{k}\right) - \frac{\alpha HL}{\beta + H} - \frac{\gamma(x)H^2}{H^2 + \eta^2}. \quad (1.20)$$

The predator equations are the same as in the habitat loss analysis, equations (1.17) and (1.19).

In the second case, the generalist saturation kill rate varies spatially (Scenario 4b), where $\gamma(x)$ is as shown in Fig. 1.2c. This function was inspired by the spatial predation rates reported in Andrén and Angelstam (1988) and the exponentially decaying predator edge incursion profile of Cantrell et al. (2002). Generalist predators were assumed to be matrix-based, with their aggregate predation rate declining to 10% that of the matrix rate (γ_m) at approximately 300 m into prey habitat. With increased habitat loss, therefore, the elevated generalist density occurs over a larger proportion of the patch. Additionally, at small enough patch sizes, γ at the center of the patch is higher than 10% of γ_m since γ decays over a shorter distance (15% of γ_m for 90% loss, 27.5% of γ_m for 95% loss). As in the first case, I investigated habitat loss at increasing generalist densities, while preserving the form of $\gamma(x)$ in Fig. 1.2c.

1.3 Results

1.3.1 Scenario 1: Northern baseline

The R-M model has a longer period of 10.8 years compared to 8.5 years for the May model at both low and high diffusivity, and the R-M predator also has a longer lag during the incline phase (Figs. 1.3 and A.1). The R-M prey has higher maximums and minimums than the May prey, while the R-M predator has lower maximums and minimums than the May predator (Tables A.1 and A.2). The May prey and predator have max/min amplitudes of 13.90 and 6.96, respectively, compared to 12.31 and 8.50 for the R-M model at high diffusivity.

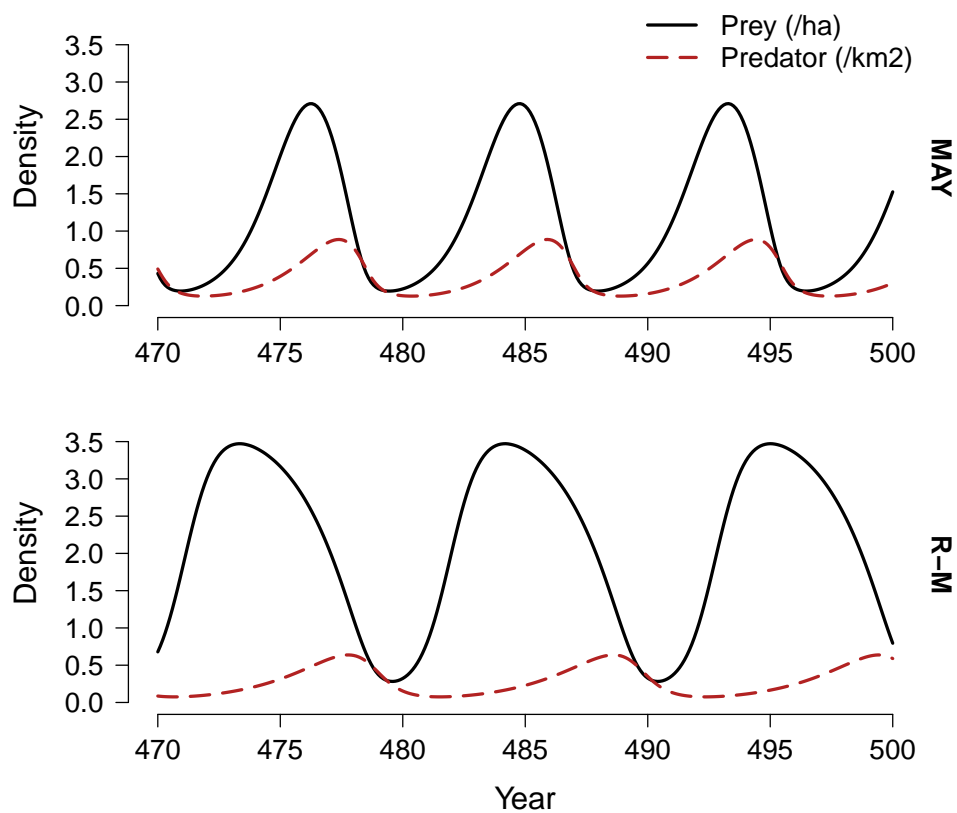


Figure 1.3: May and R-M time series at high diffusivity. The last 30 years of the 500 year simulated time series as measured in the center of a single patch at high diffusivity ($D_L = 20$ ha/yr) with no generalist predation. Parameter values are as shown in Table 1.2.

1.3.2 Scenario 2: Generalist predation

The May cycle is effectively lost at a maximum generalist predation rate of $\gamma = 0.25$ prey/ha/year (Fig. 1.4). In contrast, the R-M model stabilizes at $\gamma = 1.0$ prey/ha/year and is therefore less sensitive to generalist predation. For both models, cycle period shortens by about one year as generalist predation increases and the cycle disappears.

Generalist predation causes the limit cycles to contract inward for both models, lowering predator and prey maximums and raising minimums (Figs. 1.5a and 1.5c). For the May model, predator and prey maximums decrease substantially more than minimums rise as the limit cycles collapse into stable equilibrium points. This behavior contrasts with the R-M model, where maximums and minimums are more equally affected. Additionally, predator and prey densities approach the origin together as more generalists are added to the May system after oscillations cease, whereas the R-M predator population is extirpated first. A predation rate near $\gamma = 25$ prey/ha/year is required to bring the May predator density close to zero, but for the R-M model, the predator density goes to zero for γ between 2-3 prey/ha/year. Very large values of γ are required to bring prey densities close to zero for both models.

1.3.3 Scenario 3: Habitat loss

At low diffusivity, habitat loss initially slightly decreases May prey maximum and amplitude until approximately 60% loss (Fig. 1.4b). At this point, prey maximum and amplitude suddenly rise before sharply dropping and stabilizing at 95% loss. At high diffusion rates, the prey maximum rises more dramatically as soon as habitat is lost before dropping at 50% loss and stabilizing at 75% loss. The critical patch size for cyclicity therefore increases for the May model as animals display an increased tendency to enter the matrix. This pattern also holds for the R-M model, where oscillations cease at 80% loss at low diffusivity and 35% at high diffusivity (Fig. 1.4d). However, the R-M model is more sensitive to habitat loss than the May model both at low and high diffusivity. Moreover, the difference in critical patch size between the diffusion rates is larger for the R-M model, meaning higher movement rates exacerbate the damping effects of habitat loss even more so for the R-M

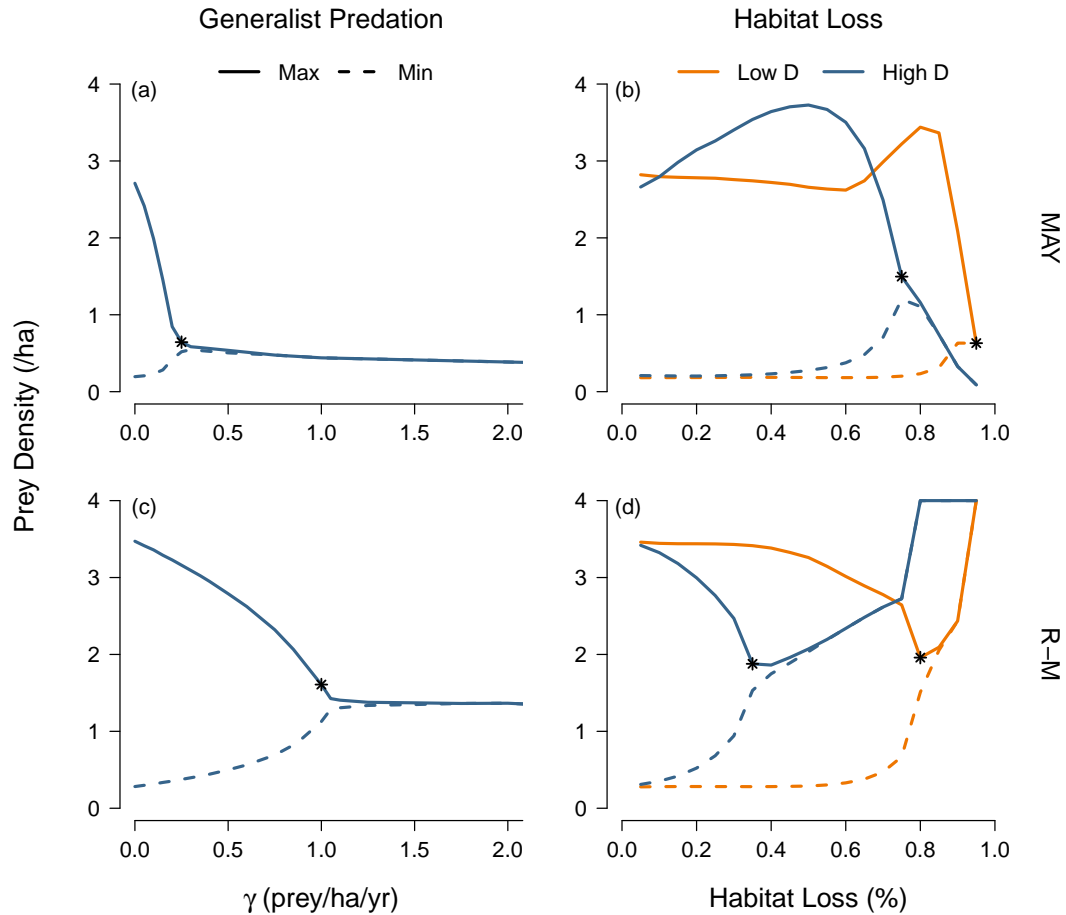


Figure 1.4: Bifurcation plots for generalist predation and habitat loss. (a) May and (c) R-M prey cycle maximum and minimum plotted as a function of γ at high diffusivity. Low diffusivity plots look almost identical. (b) May and (d) R-M prey cycle maximum and minimum plotted as a function of habitat loss percentage at low and high diffusivity. Oscillations cease where the maximum and minimum lines coalesce. The star denotes a max/min amplitude ≤ 1.5 , which is the threshold used in Tyson et al. (2010) for cyclicity. Cycles are effectively lost at $\gamma = 0.25$ for May and $\gamma = 1.0$ for R-M at both low and high diffusivity. May cycles stop at 95% habitat loss at low diffusivity and 75% loss at high diffusivity. R-M cycles stop at 80% habitat loss at low diffusivity and 35% loss at high diffusivity.

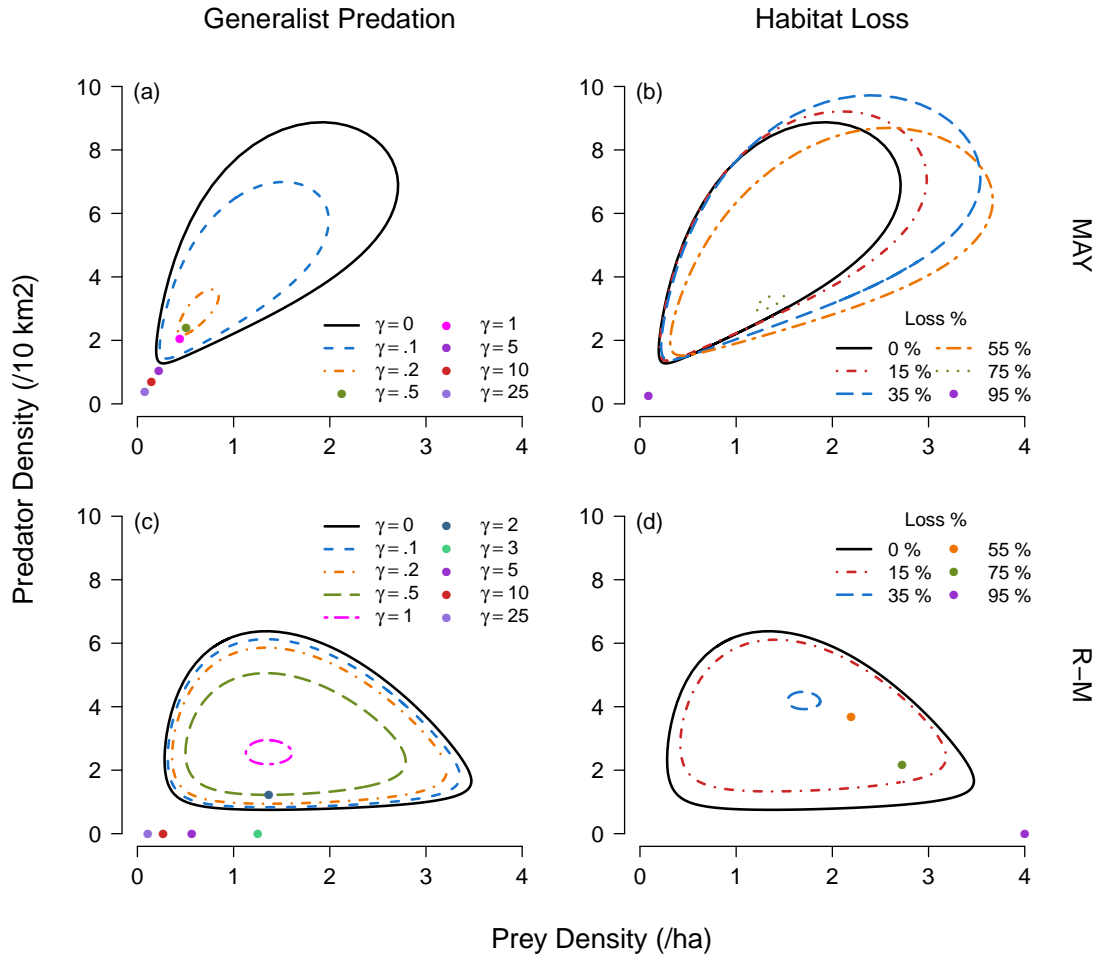


Figure 1.5: Limit cycles at varying maximum generalist predation rate and percent habitat loss at high diffusivity. Panels (a) and (c) show the effect of increasing γ on the predator-prey limit cycles for the May and R-M models, respectively, while panels (b) and (d) show the impact of habitat loss. Prey density is plotted on the x -axis, and predator density is located on the y -axis. Stable equilibrium points are represented by single points. See Appendix A.6 for low diffusivity cycles.

model. Additionally, when cycles are present, prey maximums never rise with habitat loss as in the May model.

The loss of prey habitat and subsequent decreased rate of change of the May prey population inhibits May predator growth more than the prey, resulting in decreased predation pressure that allows the prey to attain higher maximums (Fig. 1.5b, see Appendix A.4 for more). At intermediate levels of habitat loss, the predator “catches up” and also attains higher maximums until the loss is great enough to reduce predator maximums and stabilize dynamics. With increased habitat loss, May predator and prey densities approach zero. In contrast, after the RM system stabilizes, the predator is first extirpated at 95% and 80% loss for low and high diffusivity, respectively, and then the prey goes to carrying capacity. Additionally, the limit cycle contracts inwards (Fig. 1.5d), though maximums are less affected here compared to the generalist impacts. Similar to the generalist effects, the R-M period shortens by about a year as the cycle disappears. Where the limit cycle expands for the May model, period increases by up to three years.

1.3.4 Scenario 4: Generalist predation and habitat loss combined

For the May model at spatially uniform γ , I observed the same pattern as in the previous analyses, with habitat loss causing an increase in amplitude before a sudden loss of cycles, regardless of generalist predation level, and generalists continuing to have a strong damping effect (Figs. 1.6a and 1.6b). The cause of damping at low to moderate levels of habitat loss is essentially due to generalist predation because habitat loss has little effect below 60% loss at low diffusivity (Fig. 1.6a). With continued habitat loss (approximately 60-80%), the effects of generalist predation are mitigated by the relief from specialist predation. Habitat loss even causes the system to start cycling at low amplitude after being driven to stability by generalist predation. This compensatory effect of habitat loss can also be seen at high diffusivity (Fig. 1.6b), though habitat loss immediately counteracts the effects of generalist predation until approximately 40-50% loss.

Comparing matrix-based generalist predation (Fig. 1.6c) to uniformly distributed generalists (Fig. 1.6a), I found that generalist penetration into prey habitat at low diffusivity

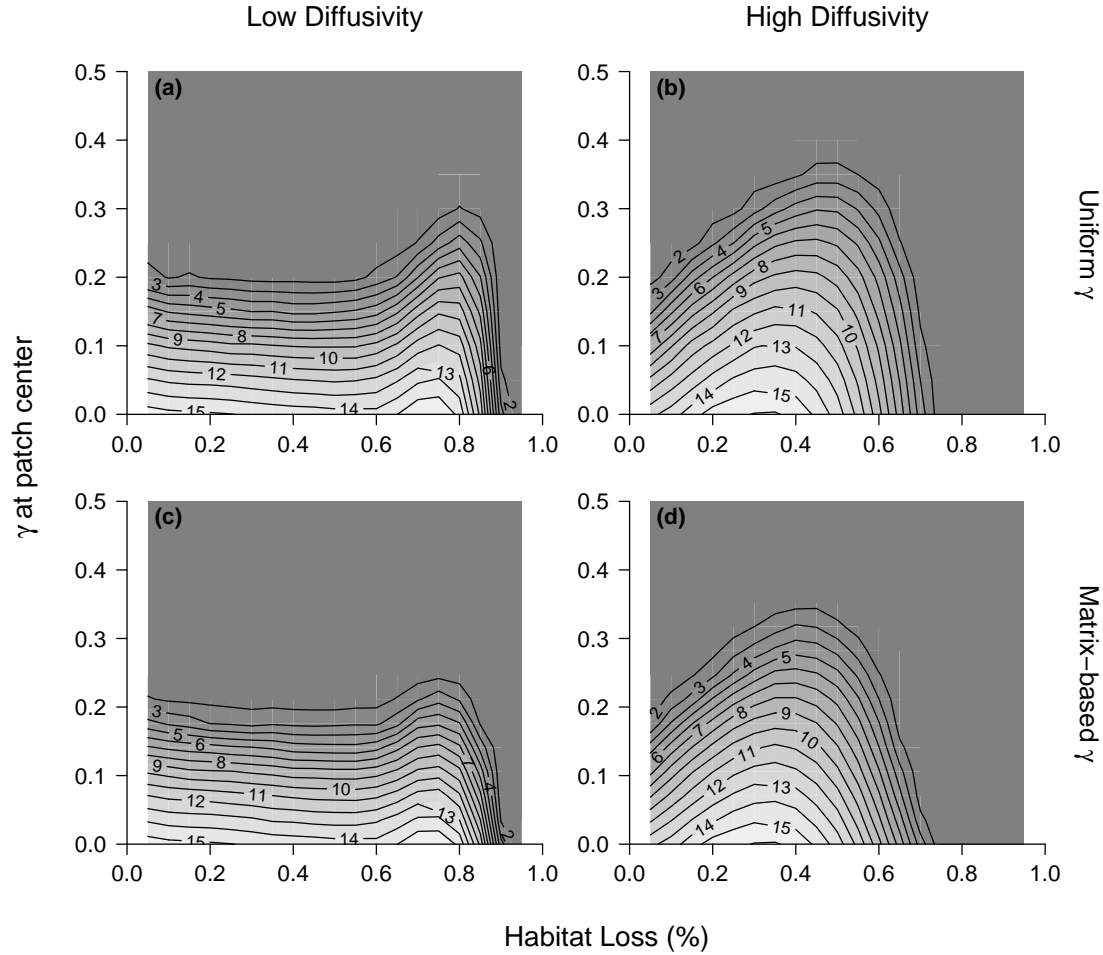


Figure 1.6: May model prey amplitude contour plots for spatially uniform and matrix-based generalists. Contour lines represent prey amplitude at the center of prey habitat computed as the ratio of cycle maximum over minimum. Panels (a) and (b) show the effect of simultaneously increasing habitat loss and spatially uniform generalist density at low and high diffusivity, respectively. Panels (c) and (d) show the effects of increasing habitat loss and matrix-based generalist densities. Percent habitat loss is shown on the x -axis, while the y -axis is the value of γ at the center of the patch, whether predation is uniform or matrix-based.

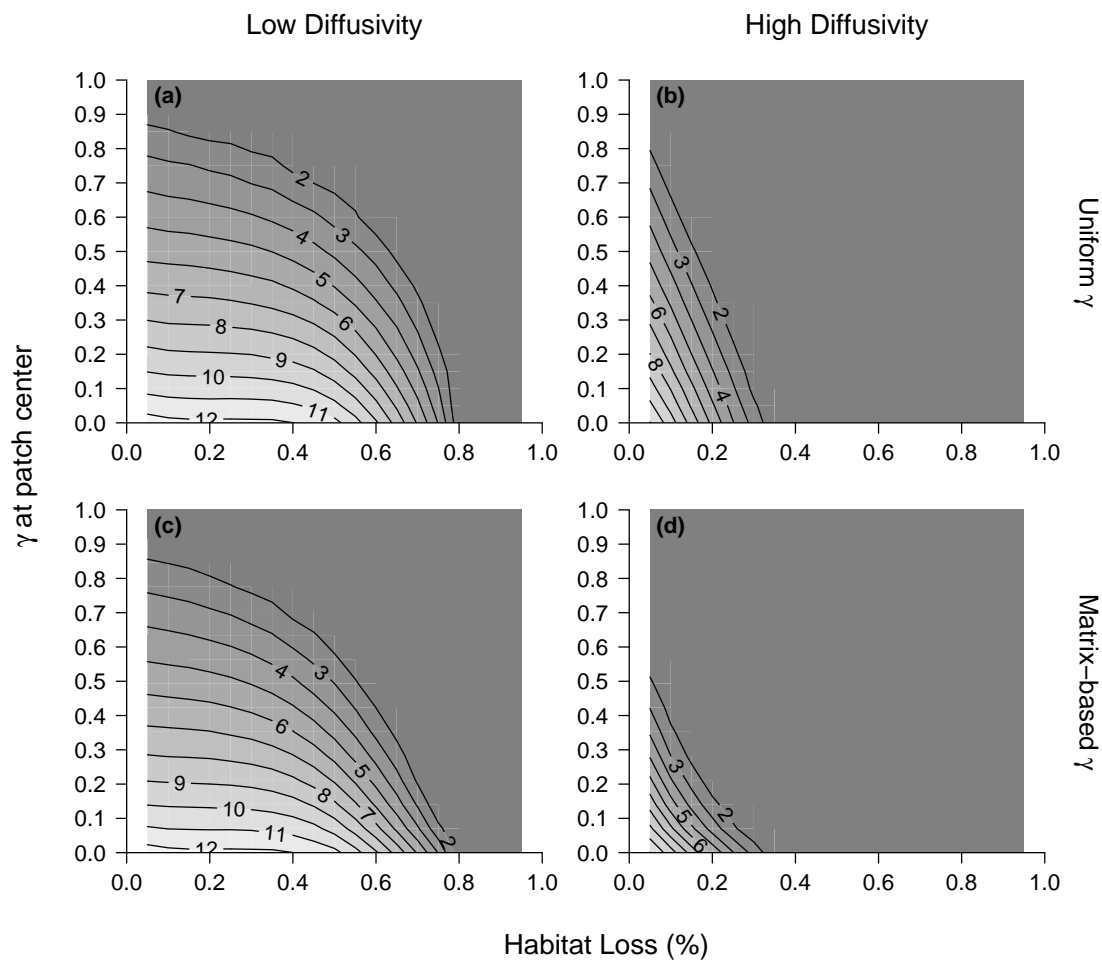


Figure 1.7: R-M model prey amplitude contour plots for spatially uniform and matrix-based generalists. Panels (a)-(d) are the same as in Fig. 1.6, with the exception that the range of γ is twice as large.

has little effect at large patch size. At smaller patch sizes, the matrix-based generalists reduce the benefit that prey receive from decreased specialist pressure as they penetrate over a larger proportion of prey habitat. At high diffusivity, the contours are slightly shifted toward the origin as generalists once again counteract the prey benefit from habitat loss, though the change is mostly overwhelmed by relief from specialist predation. At these faster movement rates, cycles do not persist at high enough habitat loss to see the impacts of elevated predation rates on very small patches.

The spatially uniform generalist contours for the R-M model also mirror the previous analyses, where the R-M prey never benefits from and amplitude decreases with habitat loss at all values of γ (Figs. 1.7a and 1.7b). The combined damping effects of habitat loss and generalist predation are additive for the R-M model; i.e. habitat loss never mitigates the generalist effects as in the May model. The R-M model remains more sensitive to habitat loss and higher diffusion rates than the May model and is less sensitive to generalist predation (note the differences in range of the γ -axes in Figs. 1.6 and 1.7).

For the R-M model, the effects of the matrix-based generalists (Fig. 1.7c) are similar to uniform predation (Fig. 1.7a) at low diffusivity and low habitat loss, as was the case with the May model. After approximately 50% habitat loss, the shape of the R-M model contours differ, where the cycle is damped faster by the matrix-based generalists as a higher proportion of the patch becomes edge. At higher diffusivity, the edge incursions change the shape of the contours immediately (Fig. 1.7d), and the elevated predation rates at patch edges further reduce the already narrow parameter range at which R-M cycles exist.

The spatial distribution of prey density differs markedly between the two models (Fig. 1.8). While not the case for most patch sizes, a patch of length 3.2 km produces similar prey cycle maximums in the center of the patch for both models, allowing a comparison of their relative densities in the matrix and at the patch edges. The R-M prey density is more uniformly distributed across the patch with high densities at the patch boundaries, whereas the May prey density is peaked in the center with much lower densities at the edges. Accordingly, the R-M prey has much higher prey density in the matrix compared to the May prey.

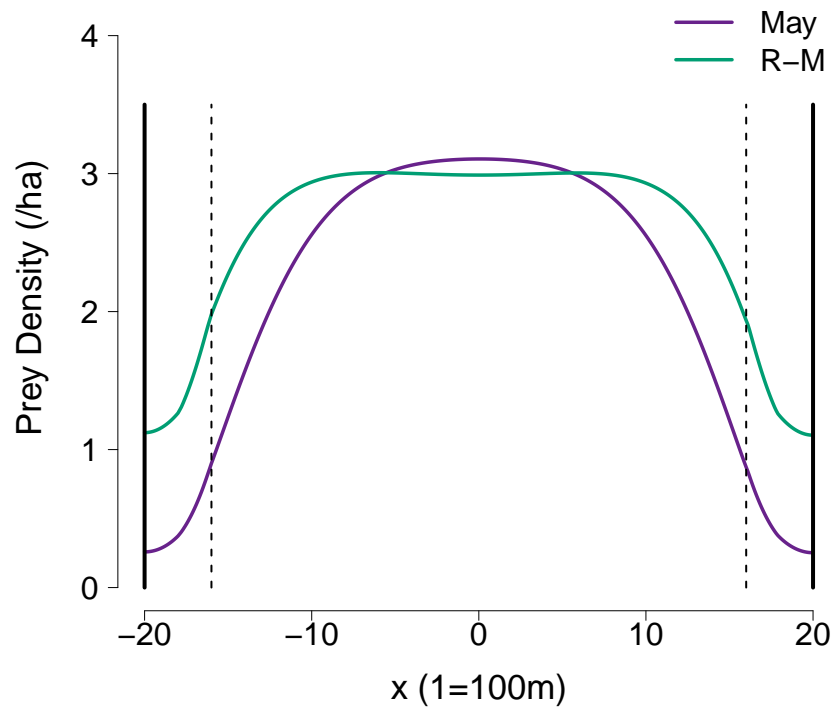


Figure 1.8: Spatial profiles of peak densities for May and R-M prey. Thick solid lines indicate the boundaries of the spatial domain. Dotted lines indicate the patch boundaries, where the center patch is 3.2 km in length. Colored solid lines show peak prey densities in space for the two models.

1.4 Discussion

Using a reaction-diffusion-advection modeling framework, I investigated how habitat loss and generalist predation affect predator-prey cycles with reaction terms taken from the May and Rosenzweig-MacArthur models. The models were parameterized using data from snowshoe hare and Canada lynx field studies to generate similar cyclic dynamics in the center of a single patch in the absence of generalist predators. I found that generalist predation has strong stabilizing effects for both models and may represent a threat to the persistence of specialized predators. The magnitude of damping from habitat loss depends on movement rates and model choice, but ultimately results in the loss of cycles. Differences in model carrying capacity may explain differences in model sensitivity to habitat loss, and cycle amplitude may or may not decrease monotonically with habitat loss, depending on model choice. Elevated generalist predation rates at patch edges and in matrix habitat hasten cycle attenuation in situations that lead to increased prey exposure to generalists, including small patch size, higher movement rates into the matrix, and increased prey density at patch edges. I review these findings and their implications below.

Scenario 1: Northern baseline

The May and R-M models do not produce identical cycles for the parameterizations used in this analysis. By constraining the spatially varying intrinsic prey growth rate to be the same for both models, while also forcing similar predator functional responses and keeping within empirical ranges for other parameters, I was unable to obtain exactly the same dynamics for two different models. However, both model parameterizations produce cycles that give reasonable population densities, amplitude, and period compared to cycles observed at Kluane Lake. The May model simulates more accurate densities for snowshoe hares compared to the R-M model, while the R-M model produces more realistic lynx densities. The most important difference between model parameterizations lies in the prey carrying capacity, where the May model required a much higher carrying capacity because the closely-following specialist is so limiting for the prey. The lower carrying capacity appears to play more of a role in initiating the cycle decline for the R-M model than the

May model, evidenced in the way the R-M prey density lingers near its peak until predator density rises substantially (Fig. 1.3). This difference in carrying capacity has important implications for model comparison (see below).

Scenario 2: Generalist predation

Generalist predation is a strong stabilizing force for both models, with the May model being more sensitive to the damping impact of generalists. For both models, predator and prey maximums decrease while minimums rise as higher generalist pressure stifles oscillations. Generalist predators are almost unresponsive at low prey densities but quite responsive at high prey densities, and they therefore serve to limit the prey peak by essentially reducing prey carrying capacity. In turn, lower prey maximums limit the maximum of the specialist predator, and lower peak predator densities mean prey troughs are not driven as low due to decreased predation pressure. Densities of noncyclic snowshoe populations do tend to be higher compared to the lows of cyclic populations (Murray 2000), so empirical patterns match the theoretical predictions of the models in this regard.

For both models, the loss of cycles occurs at rates well within the range estimated for maximum generalist predation rates at Kluane Lake, an area with cyclic populations. To produce limit cycles remotely comparable to the Kluane cycles, the maximum generalist predation rate for the May model needs to be close to the lower bound of the Kluane estimate (0.1 prey/ha/year), and the R-M model requires a rate below the mid-range value (1.0 prey/ha/year). One possible explanation is that this estimate includes removals from predators who function as specialists in Canada and actually cycle along with snowshoe hares (O'Donoghue et al. 1997, Rohner et al. 2001, Roth et al. 2007). In this case, the upper bound for the maximum generalist predation rate is likely lower. Additionally, the possibility exists that alternate parameterizations or more sophisticated models incorporating other species would be less sensitive to generalist predation.

While fewer generalists are required to stabilize the May cycle compared to the R-M cycle, the specialist predator in the R-M model is extirpated more easily by generalists after stabilization occurs. The May predator's carrying capacity is proportional to prey density,

and predators are able to persist at perhaps unrealistically low prey densities as a result. The R-M model may therefore better indicate the level of generalist predation that poses an extinction risk for a specialist predator population like the Canada lynx. The R-M model suggests that a maximum generalist predation rate between 2-3 prey/ha/year is enough to inhibit the survival of the specialist predator. The upper bound for the generalist predation rate from the Yukon is 2 prey/ha/year, which seems to imply that the lynx population has a precarious existence at Kluane Lake. While this upper bound may overestimate generalist predation rates at Kluane, as discussed above, this result does suggest that the expansion of generalist predators into northern latitudes may be a serious threat to the persistence of lynx and other specialized predators.

Scenario 3: Habitat loss

Consistent with Strohm and Tyson (2009), I found that habitat loss ultimately reduces cycle amplitude for the May and R-M models. However, I used a lower prey/predator diffusion ratio (see Appendix A.5 for a discussion) and an alternate parameterization of the R-M model, so my results differ from those of Strohm and Tyson (2009). Specifically, I found with the May model that certain levels of habitat loss increase cycle amplitude and maximum densities. Prey “benefit” from habitat loss up to a critical patch size because the predator is more negatively impacted by the loss of prey habitat than the prey itself, thus providing predation relief. Spatially-explicit metapopulation models have also found that prey may benefit from habitat loss due to a decrease in predation pressure (Swihart et al. 2001) or when prey dispersal due to predator-avoidance results in reduced rates of prey resource depletion (Prakash and de Roos 2002). However, these studies focused on presence/absence of species and did not address cycles. My results further demonstrate that a benefit to prey stemming from habitat loss can lead to higher cycle maximums and amplitudes. On the other hand, similar to Szwabiński and Pękański (2006), I showed with the R-M model that habitat loss may never benefit prey and always decrease the intensity of fluctuations in animal abundance. However, the individual-based model used in Szwabiński and Pękański (2006) did not allow for a clear identification of periodic limit cycles and the

manner in which habitat loss disrupts them.

Some similarities and differences emerged between the relative damping effects of habitat loss and generalist predation. For both models, cycle minimums rise with both habitat loss and generalist pressure, so the results from both processes match the observation noted above (Murray 2000) that southern noncyclic densities are often higher than northern cyclic lows. One key difference between the effects of generalist predation and habitat loss is that prey never benefit from generalist predation, regardless of model choice, whereas certain ranges of habitat loss can benefit prey, as discussed above with the May model. Additionally, high levels of generalist predation cause the prey population to approach zero density for both models, whereas high levels of habitat loss may either cause prey to reach carrying capacity after predator extirpation (R-M model) or cause prey and predator to stabilize and persist at low densities (May model), depending on model choice.

While it is not ecologically realistic for the prey to reach carrying capacity at high levels of habitat loss because other predators would certainly still be present, the R-M model is more useful for determining predator extirpation conditions due to the May model quirk allowing predators to persist at very low prey densities. The R-M model suggests that a low degree of habitat loss is required to stop cycles, but stable populations may still persist on patches at moderate levels of habitat loss.

R-M cycles are more sensitive to habitat loss than May cycles for the parameterizations used in this analysis. The carrying capacity of the R-M model is half that of the May model, causing differences in the logistic growth rates across the patch and in the spatial profiles (Fig. 1.8). At the center of the patch, the R-M prey peaks at a density well above its logistic inflection point and close to its carrying capacity of 4 prey/ha, so the growth rate at the center of the patch decreases substantially as the prey cycle approaches its peak. Although the form of the spatial reproduction function (Fig. 1.2) forces prey density at patch edges to be lower at the start of the cycle, the edge density catches up to the center as the cycle progresses and the growth rate declines at the center. Furthermore, at the center of the patch, the R-M prey lingers near the peak until predator numbers rise (Fig. 1.3), which further allows densities at the edge time to catch up.

In contrast, for the May model, prey density at the patch center peaks below its growth

inflection point. Prey density at the center therefore increases at an increasing rate on the cyclic incline, causing density to be more peaked here where the growth rate is highest. Additionally, the specialist predator has a shorter time lag than the R-M model and quickly drives prey density down upon peaking, leaving no time for prey to build up at patch edges. As a result of lower prey density at the edges, the May model has reduced flux of prey into the matrix. The May model therefore loses fewer prey to the matrix and is less sensitive to habitat loss. While not intentionally introduced to the two systems, this observed dynamic of lowered carrying capacity increasing the diffusive flux out of the patch is in keeping with ecological theory, where island populations pushed below carrying capacity disperse at lower rates (McKelvey et al. 2000).

Scenario 4: Generalist predation and habitat loss combined

I found that matrix-based generalists have stronger damping effects compared to uniformly distributed generalist predators in three situations, each of which lead to increased prey exposure to generalists. First, edge incursions have greater impacts with increased habitat loss as generalists encroach over a larger proportion of prey habitat. This effect is especially apparent at small patch size and low diffusivity for both models (panels (a) and (c) in Figs. 1.6 and 1.7), where edge predation reduces the predation pressure required at the patch center to damp cycles. Second, the effectiveness of matrix-based generalist predation in damping cycles increases with the inclinations of the prey and predator to move into generalist-occupied edge and matrix habitat. For both models, less habitat loss is needed to see the added damping from edge incursions at high diffusivity (panels (b) and (d) in Figs. 1.6 and 1.7) compared to low diffusivity. For instance, the low diffusivity contour plots are visibly different above 50% loss for the R-M model, whereas the high diffusivity plots substantially differ at even a low percentage of habitat loss. And third, increased prey density at patch edges increases prey susceptibility to edge predation. Edge incursions add more damping to the R-M model than the May model, most likely due to the differences in prey density at the edges (Fig. 1.8). The Type III functional response dictates higher predation rates with increased prey density (Fig. A.2), so the R-M model loses more prey

at the edges to generalist predation, even with the same functional response. In this case, prey buildup at the edges results from a lower carrying capacity and longer predator lag, but elevated prey numbers at patch edges could arise from other ecological mechanisms as well; e.g. use of edge habitats for foraging (Conroy et al. 1979, May and Norton 1996). The R-M results also demonstrate that the combination of increased movement rates into matrix habitat, high prey density at patch edges, and generalist edge incursions results in restricted parameter ranges where cycles exist (Fig. 1.7d). Cycles may therefore be unlikely in areas with these ecological features.

On the other hand, elevated predation rates at patch edges and in the matrix have little effect at large patch size, when animals have a strong inclination to stay in the patch, or when prey density is concentrated at patch centers. For systems displaying these characteristics, the extra effort to incorporate spatial differences in predation into models may be unwarranted. Similarly, predation data may only need to be collected in the heart of prey reproductive habitat for such systems, where generalist predation has its primary impact.

Finally, the May model results suggest that certain levels of habitat loss can benefit both predators and prey, even counteracting deleterious effects from generalist predators. I caution, however, that the exact degrees of habitat loss that could promote high animal densities are unclear. Even if we could accurately prescribe certain levels of loss to increase animal abundance, this dynamic is nonlinear and ultimately results in sudden and steep drops in amplitude and densities. Thus, this threshold would be difficult to predict in reality. Furthermore, we do not currently know which model better reflects reality, and the R-M model showed that a positive relationship between habitat loss and generalist predation rates may have quite strong damping impacts, and edge incursions by generalist predators may quicken the process. Therefore, perhaps the lesson to be learned is that habitat disturbances can have myriad consequences for cyclic systems that we cannot currently predict.

Future modeling

In support of the conclusions from Strohm and Tyson (2009), the differences I observed in model response to changes in landscape and the predator guild further demonstrate that

multiple models should be considered when assessing impacts on population cycles. Additionally, the consequences of model parameter choice should be carefully weighed because certain parameters (e.g. carrying capacity) may have substantial effects on dynamics when space and movement are introduced.

With regard to the modeling framework of this study, the analyses should be repeated with multiple patches of prey habitat. Simulation experiments and studies on birds and mammals in fragmented habitats (Andr en 1994) have shown that the effects of habitat fragmentation on species abundance are primarily due to habitat loss until a significant amount of habitat is destroyed. Patch size and isolation contribute to population decline at a low proportion of habitat, and this phenomenon could be incorporated in a future study to investigate fragmentation effects on cyclicity in metapopulations. Additionally, habitat interspersation and increased edge has been shown to benefit prey when they are able to dart from the edges of safer habitat into low cover but high quality food habitat, then quickly return to refuge habitat (Conroy et al. 1979, Liu et al. 2014). This trade-off between increased diversity of food resources and increased predation risk could also be investigated with this framework, similar to Liu et al. (2014). A two-dimensional spatial analysis would add to the realism and allow for additional measures of fragmentation, such as patch shape and perimeter-area ratio.

Rather than selecting parameters so that the two models produce similar cycles at the center of patch, another option would be to parameterize the models to give similar average cycles over the entire patch. This approach would not necessarily solve the problem of differing model carrying capacities, but it may be a better reflection of how data are collected and facilitate comparisons between model output and field data. Similarly, it may be more useful to look at how habitat loss and generalist predation initially perturb limit cycles instead of studying the long-term behavior of the limit cycles. This approach may provide information about the types of cycle disturbances that may occur shortly following ecological change.

Finally, certain hare predators have been shown to function closer to specialists in the Yukon, cycling along with the hare and contributing to its cyclic dynamics (O'Donoghue et al. 1997, Rohner et al. 2001). Therefore, a model incorporating multiple specialist preda-

tors similar to that of Tyson et al. (2010) may provide a better baseline for the northern dynamics. This observation also suggests that an alternate way to explore the north-south generalist predation gradient would be to change the functional response of predator species along a specialist-generalist spectrum, rather than simply increasing the number of generalist predators collectively.

Future field work

Some lynx populations in the United States may effectively operate as separate, isolated populations that, without immigration to bolster their numbers, are especially susceptible to extirpation (McKelvey et al. 2000). In this study, further habitat destruction and generalist predation caused species extirpation after the loss of cycles, so damped cycles may be a precursor to more dire consequences for cyclic species in isolated areas. In order to conserve vulnerable populations like those at the southern range boundary for lynx, we need field data that better our understanding of the relationship between habitat loss and fragmentation, generalist density and behavior, and cyclic activity. Further, we need data to assess the degree to which these factors increase the exposure of important prey species to generalist predators and contribute to the loss of cycles. Ideally, we would obtain concurrent time series data that include measures of species abundance, movement rates, predation locations and rates, and measures of habitat loss and degree of landscape fragmentation, preferably at multiple sites using the same methodology. Such data would yield better parameter estimates and clues about which models more accurately describe dynamics and which processes they should include.

With increasing human disturbances and as climate warming alters tundra landscapes (Krebs 2011), these answers will be important not just for understanding the causes for the absence of cycles in southern latitudes, but also for predicting future changes to high amplitude northern cycles. In the case of the Canada lynx, the “booms” of these northern cycles may be important for the persistence of southern populations, as the resulting dispersal maintains the geographical reach of the lynx, which is important for the viability of the species (Murray et al. 2008, Squires et al. 2013). Additionally, cyclic prey species

are often keystone herbivores in their ecosystems (Krebs 2011), and major changes to their population dynamics would have cascading ecological effects (Boutin et al. 1995).

BIBLIOGRAPHY

- Agee, J. K. 2000. Disturbance ecology of North American boreal forests and associated northern mixed/subalpine forests. *Ecology and Conservation of Lynx in the United States*. Boulder, CO: University Press of Colorado pages 39–82.
- Akçakaya, H. R. 1992. Population cycles of mammals: evidence for a ratio-dependent predation hypothesis. *Ecological Monographs* 62:119–142.
- Andrén, H. 1994. Effects of habitat fragmentation on birds and mammals in landscapes with different proportions of suitable habitat: a review. *Oikos* 71:355–366.
- Andrén, H., and P. Angelstam. 1988. Elevated predation rates as an edge effect in habitat islands: experimental evidence. *Ecology* 69:544–547.
- Andrén, H., P. Angelstam, E. Lindström, and P. Widén. 1985. Differences in predation pressure in relation to habitat fragmentation: an experiment. *Oikos* 45:273–277.
- Andrews, A. 1990. Fragmentation of habitat by roads and utility corridors: a review. *Australian Zoologist* 26:130–141.
- Batáry, P., and A. Báldi. 2004. Evidence of an edge effect on avian nest success. *Conservation Biology* 18:389–400.
- Boutin, S., C. J. Krebs, R. Boonstra, M. R. T. Dale, S. J. Hannon, K. Martin, A. R. E. Sinclair, J. N. M. Smith, R. Turkington, M. Blower, A. Byrom, F. I. Doyle, C. Doyle, D. Hik, L. Hofer, A. Hubbs, T. Karels, D. L. Murray, V. Nams, M. O’Donoghue, C. Rohner, and S. Schweiger. 1995. Population changes of the vertebrate community during a snowshoe hare cycle in Canada’s boreal forest. *Oikos* 74:69–80.
- Buskirk, S. W. 2000. Habitat fragmentation and interspecific competition: implications for lynx conservation. *Ecology and Conservation of Lynx in the United States*. Boulder, CO: University Press of Colorado pages 83–100.

- Cantrell, R. S., C. Cosner, and W. F. Fagan. 2002. Habitat edges and predator-prey interactions: effects on critical patch size. *Mathematical Biosciences* 175:31–55.
- Conroy, M. J., L. W. Gysel, and G. R. Dudderar. 1979. Habitat components of clear-cut areas for snowshoe hares in Michigan. *The Journal of Wildlife Management* pages 680–690.
- Dolbeer, R. A. 1975. Population ecology of snowshoe hares in the central Rocky Mountains. *Journal of Wildlife Management* 39:535.
- Elton, C., and M. Nicholson. 1942. The ten-year cycle in numbers of the lynx in Canada. *Journal of Animal Ecology* 11:215–244.
- Erlinge, S., J. Agrell, J. Nelson, and M. Sandell. 1992. Body weight and population dynamics: cyclic demography in a noncyclic population of the field vole (*Microtus agrestis*). *Canadian Journal of Zoology* 70:494–501.
- Gehring, T. M., and R. K. Swihart. 2003. Body size, niche breadth, and ecologically scaled responses to habitat fragmentation: mammalian predators in an agricultural landscape. *Biological Conservation* 109:283–295.
- Griffin, P. C., and S. L. Mills. 2009. Sinks without borders: snowshoe hare dynamics in a complex landscape. *Oikos* 118:1487–1498.
- Hanski, I., L. Hansson, and H. Henttonen. 1991. Specialist predators, generalist predators, and the microtine rodent cycle. *The Journal of Animal Ecology* pages 353–367.
- Harrison, S., and E. Bruna. 1999. Habitat fragmentation and large-scale conservation: what do we know for sure? *Ecography* 22:225–232.
- Hodges, K., C. Krebs, D. Hik, C. Stefan, E. Gillis, and C. Doyle. 2001. Snowshoe hare demography. *Ecosystem dynamics of the boreal forest: the Kluane project*, chapter 8 pages 141–178.

- Hodges, K. E. 2000*a*. The ecology of snowshoe hares in northern boreal forests. Ecology and Conservation of Lynx in the United States. Denver (CO): University Press of Colorado pages 117–161.
- . 2000*b*. Ecology of snowshoe hares in southern boreal and montane forests. Ecology and conservation of lynx in the United States. University Press of Colorado, Boulder, USA pages 163–206.
- Holling, C. 1959. The components of predation as revealed by a study of small-mammal predation of the European pine sawfly. *The Canadian Entomologist* 91:293–320.
- Howell, A. B. 1923. Periodic fluctuations in the numbers of small mammals. *Journal of Mammalogy* 4:149–155.
- Ives, A. R., and D. L. Murray. 1997. Can sublethal parasitism destabilize predator-prey population dynamics? a model of snowshoe hares, predators and parasites. *Journal of Animal Ecology* pages 265–278.
- Keith, L. B. 1990. Dynamics of snowshoe hare populations. *Current mammalogy* pages 119–195.
- Keith, L. B., S. E. M. Bloomer, and T. Willebrand. 1993. Dynamics of a snow shoe hare population in fragmented habitat. *Canadian Journal of Zoology* 71:1385–1392.
- King, A. A., and W. M. Schaffer. 2001. The geometry of a population cycle: a mechanistic model of snowshoe hare demography. *Ecology* 82:814–830.
- Klemola, T., M. Tanhuanpää, E. Korpimäki, and K. Ruohomäki. 2002. Specialist and generalist natural enemies as an explanation for geographical gradients in population cycles of northern herbivores. *Oikos* 99:83–94.
- Korpimäki, E., P. R. Brown, J. Jacob, and R. P. Pech. 2004. The puzzles of population cycles and outbreaks of small mammals solved? *Bioscience* 54:1071–1079.
- Krebs, C. J. 2011. Of lemmings and snowshoe hares: the ecology of northern Canada. *Proceedings of the Royal Society B: Biological Sciences* 278:481–489.

- Krebs, C. J., R. Boonstra, S. Boutin, and A. R. Sinclair. 2001*a*. What drives the 10-year cycle of snowshoe hares? *BioScience* 51:25–35.
- Krebs, C. J., S. Boutin, and R. Boonstra. 2001*b*. *Ecosystem dynamics of the boreal forest: the Kluane project*. Oxford University Press.
- Liu, R., D. DeAngelis, and J. Bryant. 2014. Dynamics of herbivores and resources on a landscape with interspersed resources and refuges. *Theoretical Ecology* 7:195–208.
- MacLulich, D. 1957. The place of change in population processes. *The Journal of Wildlife Management* pages 293–299.
- May, R. M. 2001. *Stability and complexity in model ecosystems*, vol. 6. Princeton University Press.
- May, S. A., and T. W. Norton. 1996. Influence of fragmentation and disturbance on the potential impact of feral predators on native fauna in Australian forest ecosystems. *Wildlife Research* 23:387–400.
- McKelvey, K. S., S. W. Buskirk, and C. J. Krebs. 2000. Theoretical insights into the population viability of lynx. Ruggiero, LF, KB Aubry, SW Buskirk, GM Koehler, CJ Krebs, K. S. McKelvey, and JR Squires.(Tech. Eds.). *Ecology and conservation of lynx in the United States*. Univ. Press of Colorado. Boulder, CO pages 21–37.
- Murray, D. L. 2000. A geographic analysis of snowshoe hare population demography. *Canadian Journal of Zoology* 78:1207–1217.
- Murray, D. L., T. D. Steury, and J. D. Roth. 2008. Assessment of Canada lynx research and conservation needs in the southern range: another kick at the cat. *The Journal of Wildlife Management* 72:1463–1472.
- O’Donoghue, M., S. Boutin, C. J. Krebs, and E. J. Hofer. 1997. Numerical responses of coyotes and lynx to the snowshoe hare cycle. *Oikos* 80:150–162.

- O'Donoghue, M., S. Boutin, C. J. Krebs, G. Zuleta, D. L. Murray, and E. J. Hofer. 1998. Functional responses of coyotes and lynx to the snowshoe hare cycle. *Ecology* 79:1193–1208.
- Paton, P. W. C. 1994. The effect of edge on avian nest success: How strong is the evidence? *Conservation Biology* 8:17–26.
- Prakash, S., and A. M. de Roos. 2002. Habitat destruction in a simple predator-prey patch model: how predators enhance prey persistence and abundance. *Theoretical Population Biology* 62:231–249.
- Rohner, C., F. I. Doyle, and J. N. Smith. 2001. Great horned owls. Ecosystem dynamics of the boreal forest: the Kluane project, chapter 15 pages 339–376.
- Rosenzweig, M. L., and R. H. MacArthur. 1963. Graphical representation and stability conditions of predator-prey interactions. *American Naturalist* 97:209.
- Roth, J. D., J. D. Marshall, D. L. Murray, D. M. Nickerson, and T. D. Steury. 2007. Geographic gradients in diet affect population dynamics of Canada lynx. *Ecology* 88:2736–2743.
- Ruggiero, L. F., J. R. Squires, S. W. Buskirk, K. B. Aubry, K. S. McKelvey, G. Koehler, and C. J. Krebs. 2000. Ecology and conservation of lynx in the United States. University Press of Colorado Boulder.
- Schneider, M. F. 2001. Habitat loss, fragmentation and predator impact: spatial implications for prey conservation. *Journal of Applied Ecology* 38:720–735.
- Shampine, L. F., and M. W. Reichelt. 1997. The MATLAB ODE suite. *SIAM journal on scientific computing* 18:1–22.
- Sievert, P. R., and L. B. Keith. 1985. Survival of snowshoe hares at a geographic range boundary. *The Journal of Wildlife Management* 49:854–866.

- Squires, J. R., N. J. DeCesare, L. E. Olson, J. A. Kolbe, M. Hebblewhite, and S. A. Parks. 2013. Combining resource selection and movement behavior to predict corridors for Canada lynx at their southern range periphery. *Biological Conservation* 157:187–195.
- Storch, I., E. Voitke, and S. Krieger. 2005. Landscape-scale edge effect in predation risk in forest-farmland mosaics of Central Europe. *Landscape Ecology* 20:927–940.
- Strohm, S., and R. Tyson. 2009. The effect of habitat fragmentation on cyclic population dynamics: a numerical study. *Bulletin of Mathematical Biology* 71:1323–1348.
- Strohm, S., and R. C. Tyson. 2012. The effect of habitat fragmentation on cyclic population dynamics: a reduction to ordinary differential equations. *Theoretical Ecology* 5:495–516.
- Swihart, R. K., Z. Feng, N. A. Slade, D. M. Mason, and T. M. Gehring. 2001. Effects of habitat destruction and resource supplementation in a predator-prey metapopulation model. *Journal of Theoretical Biology* 210:287–303.
- Szwabiński, J., and A. Pękalski. 2006. Effects of random habitat destruction in a predator-prey model. *Physica A: Statistical Mechanics and its Applications* 360:59–70.
- Taylor, R. A., A. White, and J. A. Sherratt. 2013. How do variations in seasonality affect population cycles? *Proceedings of the Royal Society B: Biological Sciences* 280:20122714.
- Turchin, P. 2003. *Complex population dynamics: a theoretical/empirical synthesis*, vol. 35. Princeton University Press.
- Turchin, P., and I. Hanski. 1997. An empirically based model for latitudinal gradient in vole population dynamics. *The American Naturalist* 149:842–874.
- Tyson, R., S. Haines, and K. E. Hodges. 2010. Modelling the Canada lynx and snowshoe hare population cycle: the role of specialist predators. *Theoretical Ecology* 3:97–111.
- Ward, R. M., and C. J. Krebs. 1985. Behavioural responses of lynx to declining snowshoe hare abundance. *Canadian Journal of Zoology* 63:2817–2824.
- Wilcove, D. S. 1985. Nest predation in forest tracts and the decline of migratory songbirds. *Ecology* 66:1211–1214.

- Wirsiing, A. J., T. D. Steury, and D. L. Murray. 2002. A demographic analysis of a southern snowshoe hare population in a fragmented habitat: evaluating the refugium model. *Canadian Journal of Zoology* 80:169–177.
- Wolff, J. O. 1980. The role of habitat patchiness in the population dynamics of snowshoe hares. *Ecological Monographs* 50:111–130.

Appendix A

SUPPLEMENTARY MATERIAL

A.1 Spatial functions

Below are details regarding the spatially varying prey growth rate, velocity, and matrix-based generalist predation functions.

A.1.1 Prey reproduction function

The prey intrinsic growth rate, r , for both the May and R-M models varies spatially, consistent with the methods of Strohm and Tyson (2009). The function $r(x)$ is defined piecewise over the spatial grid, where $r(x) = 0$ outside of the center patch of prey habitat. On the patch of prey habitat, the left half of the function is defined as

$$r(x) = r \left[\frac{2}{\pi} \tan^{-1}[(x + L_h/2)/dx] \right], \quad x \in \left[-\frac{L_h}{2}, \dots, -0.2, -0.1, 0 \right], \quad (\text{A.1})$$

and the right half as

$$r(x) = r \left[-\frac{2}{\pi} \tan^{-1}[(x - L_h/2)/dx] \right], \quad x \in \left[0, 0.1, 0.2, \dots, \frac{L_h}{2} \right], \quad (\text{A.2})$$

where $dx = 0.1 = 10$ m is the spatial step size used, and L_h is the length of the patch of habitat, which is measured in 100 m units and centered at $x = 0$. Values of x that do not lie exactly on the grid are mapped to the closest grid point. The function is scaled so that the growth rate attains its maximum, $r = 1.75$, precisely in the center of the patch, regardless of patch size.

A.1.2 Prey and predator velocity function

The same velocity function was used for both the predator and prey for consistency with Strohm and Tyson (2009). The function $V(x)$ is defined piecewise over the spatial grid,

where $V(x) = 0$ in prey habitat and on the outer halves of the matrix. In the matrix to the left of the prey habitat, the function is defined as

$$V(x) = 0, \quad x \in \left[-20, -19.9, \dots, -20 + \frac{L_m}{2}\right], \quad (\text{A.3})$$

$$V(x) = r \left[\frac{2}{\pi} \tan^{-1}[(x + 20 - L_m/2)/dx] \right], \quad x \in \left[-20 + \frac{L_m}{2}, -19.9 + \frac{L_m}{2}, \dots, -20 + \frac{3L_m}{4}\right], \quad (\text{A.4})$$

$$V(x) = r \left[-\frac{2}{\pi} \tan^{-1}[(x + 20 - L_m)/dx] \right], \quad x \in \left[-20 + \frac{3L_m}{4}, -19.9 + \frac{3L_m}{4}, \dots, -20 + L_m\right], \quad (\text{A.5})$$

where L_m is the length of each matrix area, measured in 100 m units. In the matrix to the right of the prey habitat, the function is defined as

$$V(x) = r \left[-\frac{2}{\pi} \tan^{-1}[(x - 20 + L_m)/dx] \right], \quad x \in \left[20 - L_m, 20.1 - L_m, \dots, 20 - \frac{3L_m}{4}\right], \quad (\text{A.6})$$

$$V(x) = r \left[\frac{2}{\pi} \tan^{-1}[(x - 20 + \frac{L_m}{2})/dx] \right], \quad x \in \left[20 - \frac{3L_m}{4}, 20.1 - \frac{3L_m}{4}, \dots, 20 - \frac{L_m}{2}\right], \quad (\text{A.7})$$

$$V(x) = 0, \quad x \in \left[20 - \frac{L_m}{2}, 20.1 - \frac{L_m}{2}, \dots, 20\right]. \quad (\text{A.8})$$

A.1.3 Matrix-based generalist function

The matrix-based generalist predation function, $\gamma(x)$, was inspired by the edge predation work of Andr en and Angelstam (1988). An exponentially decaying function was fit to the approximate data reported in Andr en and Angelstam (1988), while forcing the predation rate in prey habitat to asymptote at 10% of the matrix predation rate, γ_m , for simplicity. The exponential decay starts at 30 m outside of prey habitat. For the left half of the landscape, the function is defined as

$$\gamma(x) = \gamma_m, \quad x \in [-20, -19.9, \dots, -20.3 + L_m], \quad (\text{A.9})$$

$$\gamma(x) = \gamma_m \left(.1 + e^{-0.48013 - 0.001263 \left[\frac{x+20-L_m}{dx} \right]} \right), \quad x \in [-20.2 + L_m, -20.1 + L_m, \dots, 0], \quad (\text{A.10})$$

where L_m is the length of each matrix area, measured in 100 m units. The right half of the landscape is the mirror image of this function.

A.2 Northern baseline dynamics

The simulated time series at low diffusivity (Fig. A.1) looks very similar to the time series at high diffusivity (Fig. 1.3), though higher diffusion rates do slightly reduce maximum densities and amplitude (Tables A.1 and A.2).

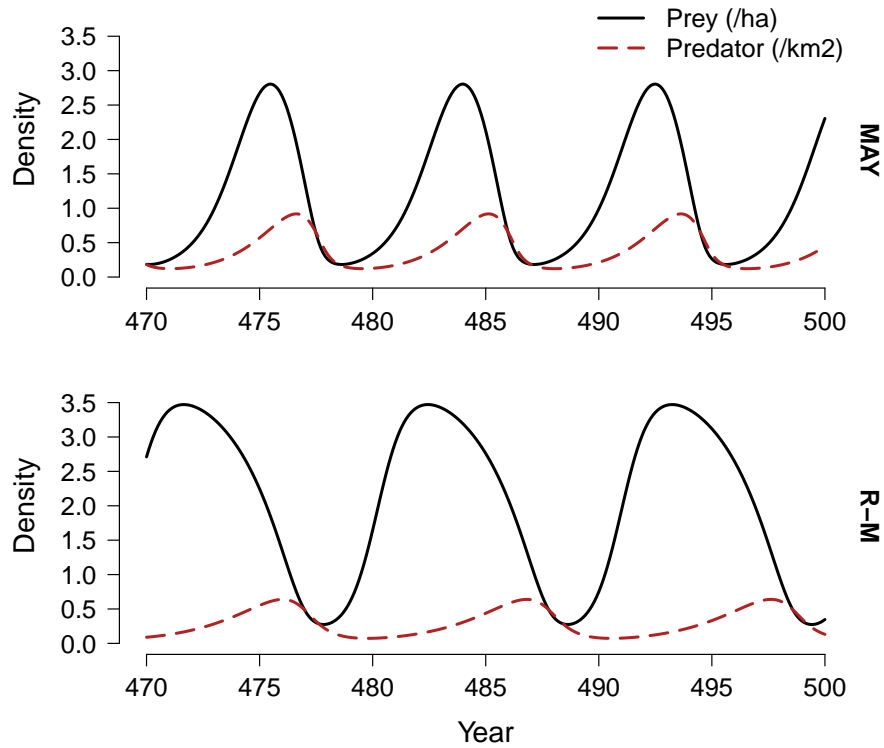


Figure A.1: May and R-M time series at low diffusivity. The last 30 years of the 500 year simulated time series as measured in the center of a single patch at low diffusivity ($D_L = 2$ ha/yr) with no generalist predation. Parameter values are as shown in Table 1.2.

Table A.1: Prey and predator cycle attributes for the May and R-M models on a single patch at high diffusivity. Attributes are measured in the center of the single patch without generalist predators over the last 30 years of a 500 year simulated time series. Prey maximums and minimums have units prey/ha and predator maximums and minimums have units predators/10 km². Amplitudes computed as the difference between maximums and minimums inherit the corresponding units. Amplitudes computed as the quotient between maximums and minimums are dimensionless. Period is measured in years. Cycle attributes are shown for prey/predator diffusion ratio $D = \frac{D_H}{D_L} = .50$ and a “high” predator diffusivity of $D_L = 20$ ha/yr.

Model	Max	Min	Amplitude (Max-Min)	Amplitude (Max/Min)	Period
May PREY	2.71	0.19	2.51	13.90	8.5
R-M PREY	3.47	0.28	3.19	12.31	10.85
May PREDATOR	8.87	1.27	7.60	6.96	8.5
R-M PREDATOR	6.38	0.75	5.63	8.5	10.85

Table A.2: Prey and predator cycle attributes for the May and R-M models on a single patch at low diffusivity. Attributes are measured in the center of the single patch without generalist predators over the last 30 years of a 500 year simulated time series. Units are as described in Table A.1 above. Cycle attributes are shown for prey/predator diffusion ratio $D = \frac{D_H}{D_L} = .50$ and a “low” predator diffusivity of $D_L = 2$ ha/yr.

Model	Max	Min	Amplitude (Max-Min)	Amplitude (Max/Min)	Period
May PREY	2.81	0.18	2.62	15.35	8.5
R-M PREY	3.47	0.27	3.20	12.65	10.8
May PREDATOR	9.18	1.22	7.96	7.55	8.5
R-M PREDATOR	6.39	0.73	5.66	8.76	10.8

A.3 Type III functional response

For this analysis, the half-saturation constant, η , of the Holling Type III functional response for generalist predators was held constant at 1.25 prey/ha, but the maximum generalist predation rate, γ , varied (Fig. A.2). The saturation kill rate may also be written as $\gamma = \hat{\gamma}G$, where $\hat{\gamma}$ is the average maximum number of prey each generalist predator can kill per year, and G is the density of generalist predators. An increase in γ is therefore equivalent to an increase in the density (G), the average predation capacity ($\hat{\gamma}$) of the generalist predators, or both. For the purpose of this study, an increase in γ was viewed as an increase in the density of generalist predators while holding their average predation capacity constant.

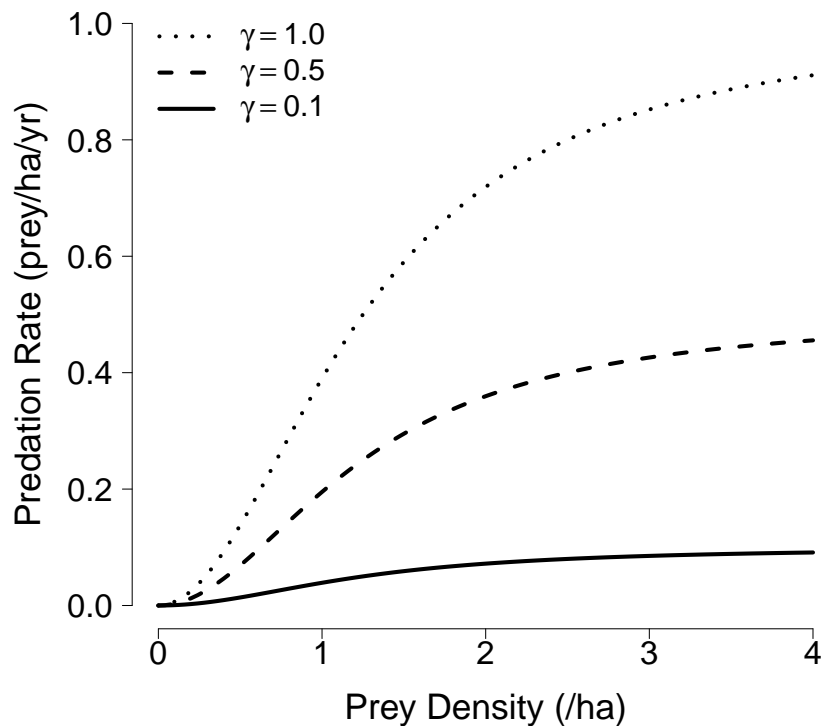


Figure A.2: Generalist Type III functional response. The effect of increasing the maximum generalist predation rate, γ , on the Type III response while holding the half-saturation constant, η , fixed at 1.25 prey/ha.

A.4 Habitat loss and predator velocity

Predator velocity does not qualitatively change the habitat loss results, but setting the predator's velocity to zero does lend further support to the notion that relief from specialist predation is behind the observed increase in amplitude for the May model. Where prey maximum increases with habitat loss, a bigger increase is obtained by removing the predator velocity term (Figs. A.3a and A.4a). Zero velocity means fewer predators are drawn to prey habitat, resulting in decreased predation rates on the patch. This additional relief in predation allows the prey to attain even higher maximums compared to the non-zero velocity function used in the habitat loss analysis. Interestingly, where prey maximum and amplitude decrease with habitat loss, increased predator presence on the patch raises the maximum and amplitude for both models (Figs. A.3 and A.4).

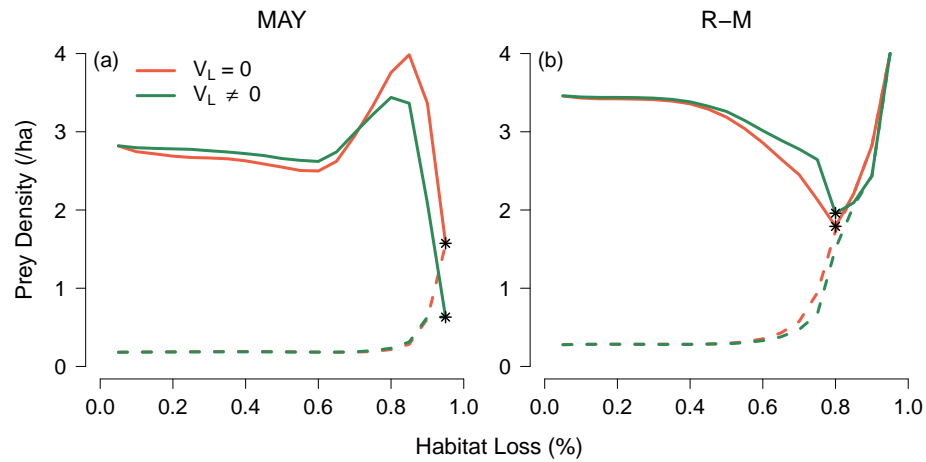


Figure A.3: Bifurcation plots with and without predator velocity at low diffusivity. (a) May and (b) R-M prey cycle maximum and minimum plotted as a function of habitat loss percentage, where $V_L = 0$ is without a predator velocity function, and $V_L \neq 0$ is with a predator velocity function. Oscillations cease where the maximum and minimum lines coalesce. The star denotes a max/min amplitude ≤ 1.5 . Demographic parameter values are in Table 1.2.

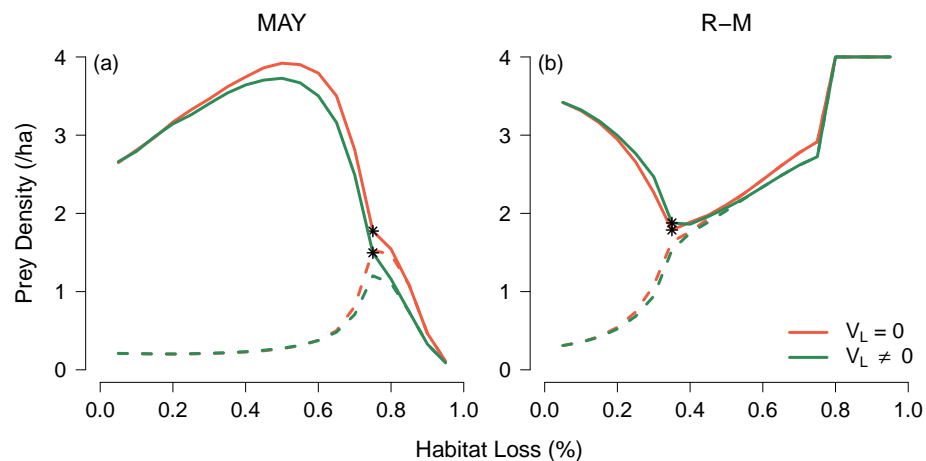


Figure A.4: Bifurcation plots with and without predator velocity at high diffusivity. Same as Fig. A.3 but at high diffusivity.

A.5 *Habitat loss and diffusion ratio*

While prey/predator diffusion ratio makes little difference on a single patch (Appendix B.1), the ratio does make a difference when habitat is lost. For the R-M model, the diffusion ratio has little effect at low diffusivity (Fig. A.5b), but increased tendency of the predator to move into the matrix relative to the prey decreases cycle amplitude at high diffusivity (Fig. A.6b). As in Appendix A.4, predator presence on the patch seems to contribute to cyclicity for the R-M model.

The ratio has a bigger impact for the May model and determines whether amplitude will increase with habitat loss. Prey maximums increase as the predator has a stronger inclination to enter the matrix than the prey (i.e. as D decreases), which causes decreased predation rates on the patch as in Appendix A.4 (Figs. A.5a and A.6a). Strohm and Tyson (2009) likely did not observe this increase in amplitude because they used low diffusivity, and their prey and predator diffusion rates were closer to each other ($D = .75$ in Fig. A.5a).

In Fig. A.5, the ratio $D = .25$ is not shown because *pdepe* failed to find a solution for the May model after oscillations ceased, resulting in an incomplete graph. This particular diffusion ratio results in very strange dynamics for the May model (Fig. A.6a). Cycles are first lost at 10% habitat loss, then resume in a very big way between 25-70% loss.

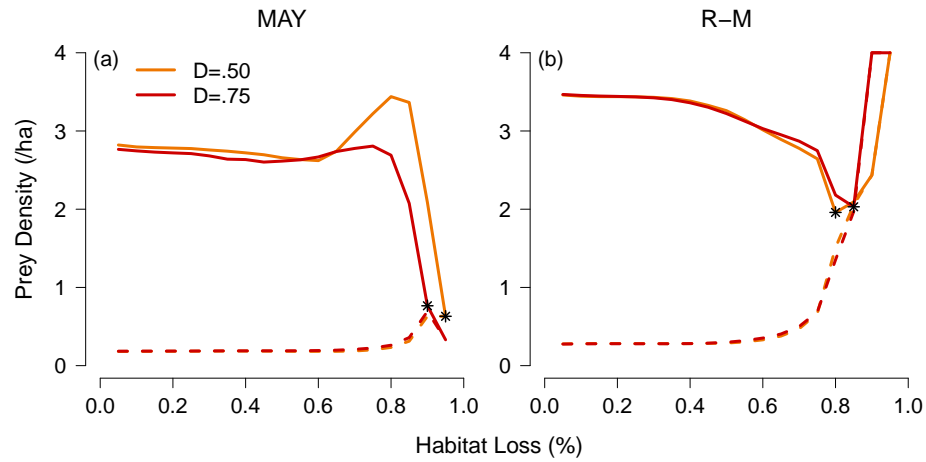


Figure A.5: Bifurcation plots at varying diffusion ratios at low diffusivity. (a) May and (b) R-M prey cycle maximum and minimum plotted as a function of habitat loss percentage, where $D = \frac{D_H}{D_L}$ and $D_L = 2$ ha/yr. Oscillations cease where the maximum and minimum lines coalesce. The star denotes a max/min amplitude ≤ 1.5 . Demographic parameter values are in Table 1.2.

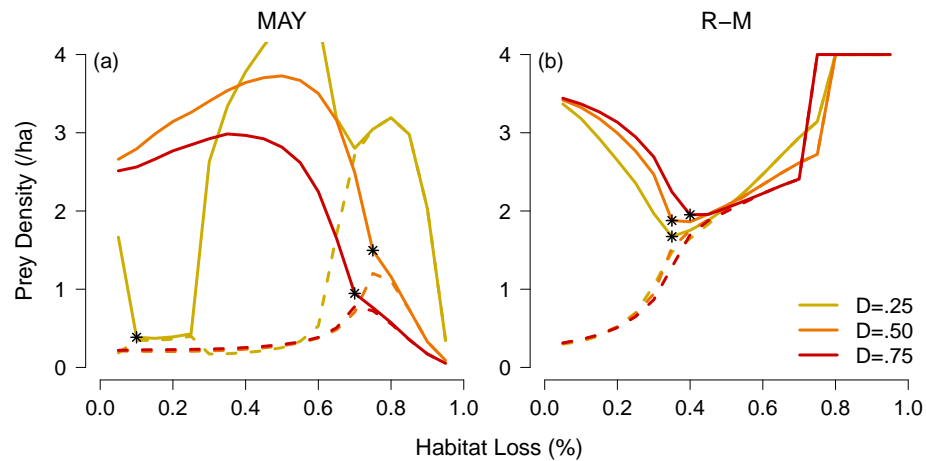


Figure A.6: Bifurcation plots at varying diffusion ratios at high diffusivity. Same as Fig. A.5 but at high diffusivity ($D_L = 20$ ha/yr). The maximum for $D = .25$ is slightly cut off in panel (a) for the prey density limits used in all other figures.

A.6 *Limit cycles at low diffusivity*

The impacts of generalist predation on the model limit cycles are very similar at low diffusivity (Figs. A.7a and A.7c) and high diffusivity (Figs. 1.5a and 1.5c), though the cycles have slightly larger amplitude at low diffusivity. Additionally, more habitat loss is required to damp cycles at low diffusivity for both models. More habitat loss is required for the May prey to experience predation relief at low diffusivity (Fig. A.7b), and the R-M predator persists at a higher proportion of habitat loss at low diffusion rates (Fig. A.7d).

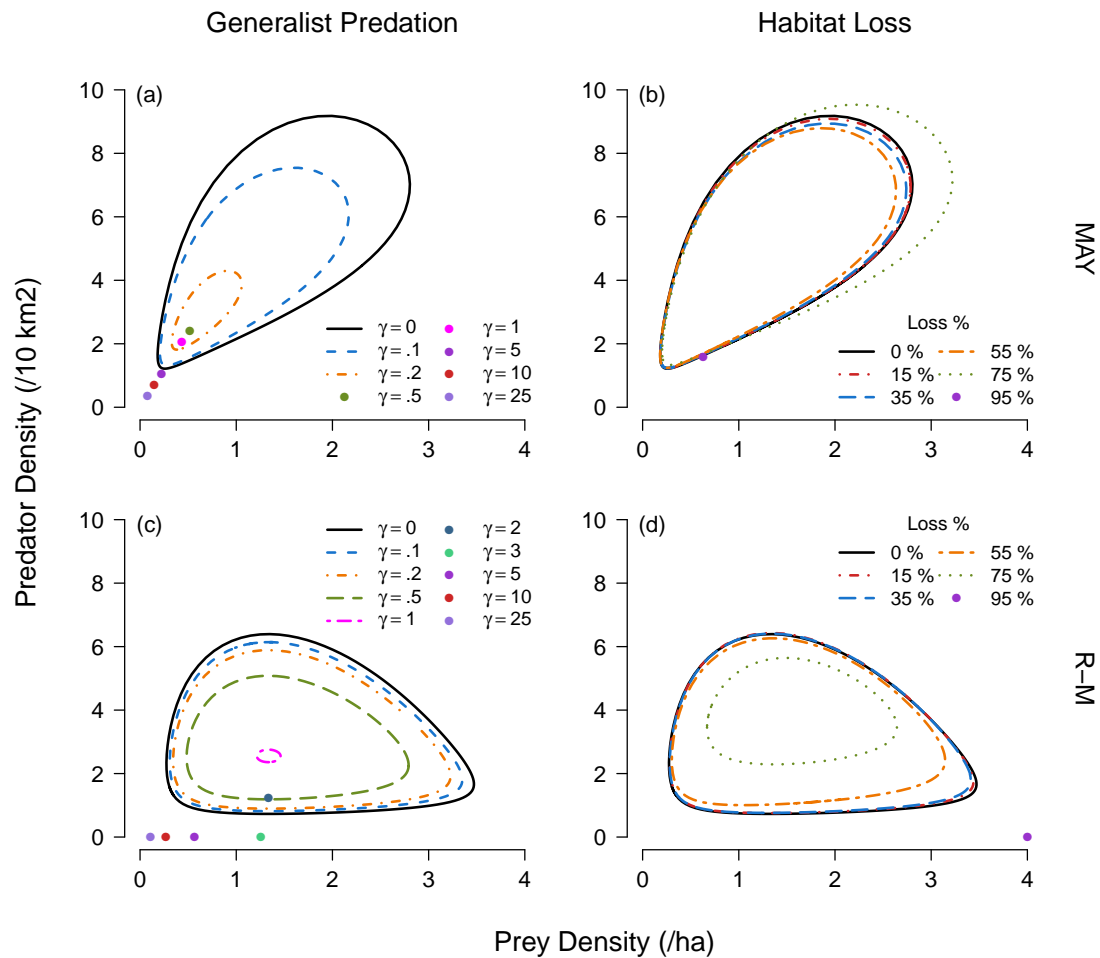


Figure A.7: Limit cycles at varying maximum generalist predation rate and percent habitat loss at low diffusivity. Panels (a) and (c) show the effect of increasing γ on the predator-prey limit cycles for the May and R-M models, respectively, while panels (b) and (d) show the impact of habitat loss. Prey density is plotted on the x -axis, and predator density is located on the y -axis. Stable equilibrium points are represented by single points.

Table B.2: Impacts of increasing predator diffusivity on R-M prey and predator cycle attributes in the center of a single patch without generalist predation at $D = \frac{D_H}{D_L} = .75$ and $D = .5$. Parameter values can be found in Table 1.2. (diff) denotes amplitude computed as the difference between maximum and minimum, and (ratio) denotes amplitude computed as the ratio of maximum over minimum.

Attribute	$D_L (D = .75)$				$D_L (D = .5)$			
	2	4	8	20	2	4	8	20
Prey Max	3.47	3.45	3.47	3.47	3.47	3.47	3.45	3.47
Prey Min	0.27	0.28	0.28	0.28	0.27	0.28	0.28	0.28
Predator Max	6.39	6.37	6.39	6.38	6.39	6.39	6.37	6.38
Predator Min	0.73	0.75	0.74	0.75	0.73	0.73	0.76	0.75
Prey Amp (diff)	3.2	3.17	3.19	3.19	3.2	3.19	3.17	3.19
Prey Amp (ratio)	12.65	12.25	12.57	12.29	12.65	12.6	12.24	12.31
Predator Amp (diff)	5.66	5.62	5.65	5.63	5.66	5.66	5.61	5.63
Predator Amp (ratio)	8.77	8.45	8.63	8.54	8.76	8.71	8.39	8.5
Period	10.8	10.75	10.8	10.8	10.8	10.75	10.75	10.85

B.2 Generalist predation and diffusion

The magnitude of diffusivity (D_L) and the prey/predator diffusion ratio (D) have no effect on the maximum generalist predation rate that stabilizes cycles (γ_s) for the R-M model, whether amplitude is computed as the difference or ratio between maximum and minimum (Table B.3). For the May model, γ_s slightly changes with D_L at $D = .5$ when amplitude is computed as the difference between maximum and minimum, though it is constant with respect to D_L at $D = .75$. When amplitude is computed as a ratio, γ_s does not change with diffusivity or diffusion ratio.

Table B.3: Critical maximum generalist predation rates for cyclicity for the May and R-M models as diffusivity increases at prey/predator diffusion ratios $D = \frac{D_H}{D_L} = .75$ and $D = .5$. (diff) denotes amplitude computed as the difference between maximum and minimum, where γ_s is the maximum generalist predation rate at which the difference is ≤ 0.1 . (ratio) denotes amplitude computed as the ratio of maximum over minimum, where γ_s is the maximum generalist predation rate at which the ratio is ≤ 1.5 .

Critical Value	$D_L (D = .75)$				$D_L (D = .5)$			
	2	4	8	20	2	4	8	20
May γ_s (diff)	.30	.30	.30	.30	.35	.30	.25	.30
May γ_s (ratio)	.25	.25	.25	.25	.25	.25	.25	.25
R-M γ_s (diff)	1.1	1.1	1.1	1.1	1.1	1.1	1.1	1.1
R-M γ_s (ratio)	1.0	1.0	1.0	1.0	1.0	1.0	1.0	1.0

B.3 Habitat loss and matrix velocity

For consistency, the velocity function was defined similarly to that of Strohm and Tyson (2009), where the velocity is zero over the outer halves of the two areas of matrix habitat. That is, the velocity term only pulls animals towards the patch when they are in matrix habitat close to prey habitat. Another way to define the function is to have the velocity term draw animals towards prey habitat over the whole matrix area, rather than over half of it. I looked at this alternate definition for the velocity function, and it did not affect results for the habitat loss analysis (Figs. B.1 and B.2).

At small patch size, the outer halves of the matrix area have very low prey density (add a figure if time), and the additional flux of prey towards the center is therefore negligible. At larger patches of prey habitat, there is higher density in the outer edges (Fig. 1.8), but the additional flux of prey is outweighed by the vastness of the patch and has little effect on the density at the center of the patch.

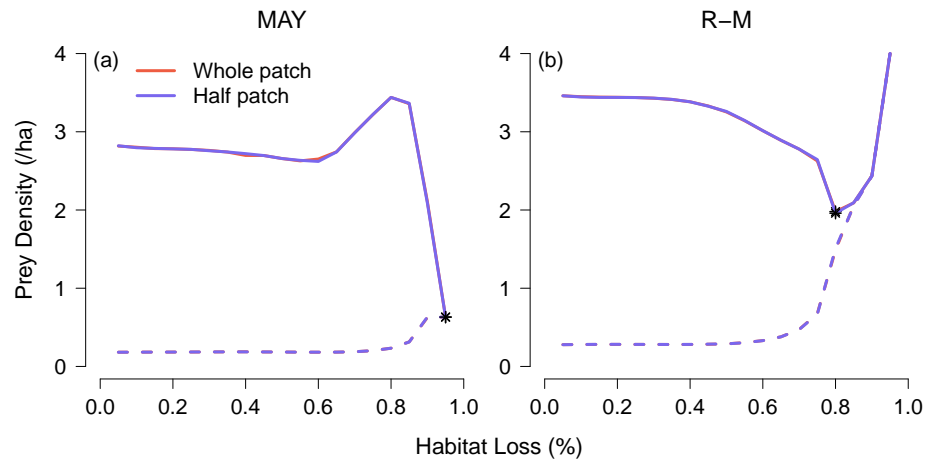


Figure B.1: Bifurcation plots for two velocity functions at low diffusivity. (a) May and (b) R-M prey cycle maximum and minimum plotted as a function of habitat loss percentage, where ‘Whole patch’ refers to the non-zero velocity function over the whole matrix, and ‘Half patch’ refers to the function used in this thesis with zero velocity on the outer halves of the matrix. Oscillations cease where the maximum and minimum lines coalesce. The star denotes a max/min amplitude ≤ 1.5 . Demographic parameter values are in Table 1.2.

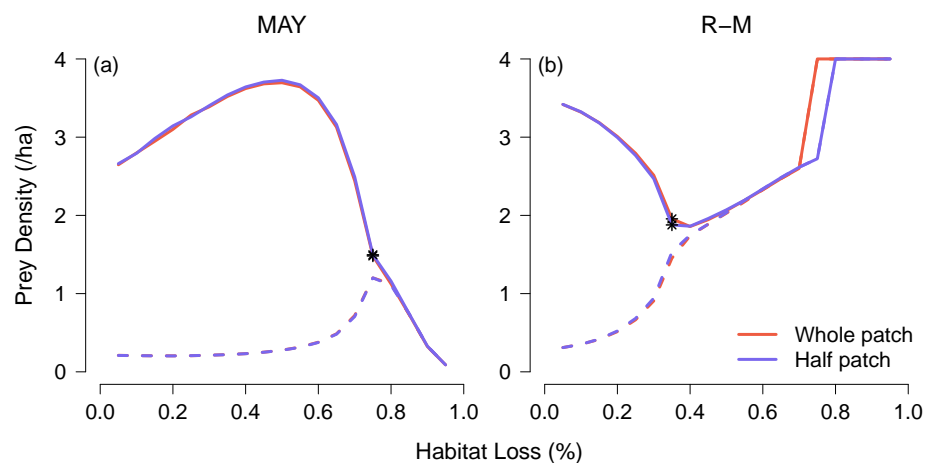


Figure B.2: Bifurcation plots for two velocity functions at high diffusivity. Same as Fig. B.1 but at high diffusivity.